

## QUALITATIVE INTERPRETATION OF GALAXY SPECTRA

J. SÁNCHEZ ALMEIDA<sup>1,2</sup>, R. TERLEVICH<sup>3,4</sup>, E. TERLEVICH<sup>3</sup>, R. CID FERNANDES<sup>5</sup>, A. B. MORALES-LUIS<sup>1,2</sup>*Draft version February 26, 2024*

## ABSTRACT

We describe a simple step-by-step guide to qualitative interpretation of galaxy spectra (Fig. 11). Rather than an alternative to existing automated tools, it is put forward as an instrument for quick-look analysis, and for gaining physical insight when interpreting the outputs provided by automated tools. Though the recipe is of general application, it was developed for understanding the nature of the Automatic Spectroscopic K-means based (ASK) template spectra. They resulted from the classification of all the galaxy spectra in the Sloan Digital Sky Survey data release 7 (SDSS-DR7), thus being a comprehensive representation of the galaxy spectra in the local universe. Using the recipe, we give a description of the properties of the gas and the stars that characterize the ASK classes, from those corresponding to passively evolving galaxies, to HII galaxies undergoing a galaxy-wide starburst. The qualitative analysis is found to be in excellent agreement with quantitative analyses of the same spectra. We compare the mean ages of the stellar populations with those inferred using the code STARLIGHT. We also examine the estimated gas-phase metallicity with the metallicities obtained using electron-temperature based methods. A number of byproducts follow from the analysis. There is a tight correlation between the age of the stellar population and the metallicity of the gas, which is stronger than the correlations between galaxy mass and stellar age, and galaxy mass and gas metallicity. The galaxy spectra are known to follow a 1-dimensional sequence, and we identify the luminosity-weighted mean stellar age as the affine parameter that describes the sequence. All ASK classes happen to have a significant fraction of old stars, although spectrum-wise they are outshined by the youngest populations. Old stars are metal rich or metal poor depending on whether they reside in passive galaxies or in star-forming galaxies.

*Subject headings:* methods: data analysis – atlases – galaxies: evolution – galaxies: general

## 1. INTRODUCTION

There are several automated tools for inferring the properties of the stellar populations contributing to the integrated galaxy spectra. The list includes MOPED (Panter et al. 2004), STARLIGHT (Cid Fernandes et al. 2005), STECKMAP (Ocvirk et al. 2006), VESPA (Tojeiro et al. 2007), or ULYSS (Koleva et al. 2009), as well as the use of line indices like the Lick indices (Worthey et al. 1994). Similarly, there are semi-automatic procedures to deduce the properties of the gas (e.g., Shaw & Dufour 1995; Johnson et al. 2006; Luridiana et al. 2011), including the so-called strong-line ratio methods (e.g., Pagel et al. 1979; Díaz & Pérez-Montero 2000; Denicoló et al. 2002; Shi et al. 2005). These tools are (and will be) fundamental for understanding the galaxy formation and evolution, but the blind use of the codes results quite unsatisfactory from a physical stand point. One obtains a precise quantitative description of the stellar populations contributing to the integrated spectra, but ignores the reason why the code has chosen them

rather than other potential alternatives. The educated eye of an astronomer is often far more telling from a physical point of view. Unfortunately, the know-how of qualitatively interpreting a spectrum is learned after a long experience of working in the field. The information on which particular spectral feature informs of which particular physical property is scattered among a large number of technical publications, difficult to identify and to deal with for a newcomer. This paper aims at providing a step-by-step guide to qualitative interpretation of galaxy spectra. Moreover, it will be compared with up-to-date numerical techniques to show that both qualitative and quantitative results are in excellent agreement.

The work was originally planned as a mere academic exercise to understand the nature of the classes resulting from the k-means classification of all the galaxy spectra in the Sloan Digital Sky Survey data release 7 (SDSS-DR7, Sánchez Almeida et al. 2010). We wanted to translate the spectral shapes into physical units like stellar ages and metallicities, so that this information can be used to tailor class-based searches (e.g., Ammerl et al. 2012), or when interpreting spectra (e.g., Sánchez-Janssen et al. 2012). However, the exercise is of interest beyond the original scope. The simple decision tree we use is suitable to characterize any galaxy spectrum. We know of its generality because it allows to separate and characterize the 28 Automated Spectroscopic K-means-based (ASK) classes (Sánchez Almeida et al. 2010) which, by construction, are proxies that condense the properties of the some one-million SDSS spectra (Stoughton et al. 2002; Abazajian et al. 2009). The ASK

jos@iac.es, rjt@ast.cam.ac.uk, eterlevi@inaoep.mx, cid@astro.ufsc.br, abazajian@ucsd.edu

<sup>1</sup> Instituto de Astrofísica de Canarias, E-38205 La Laguna, Tenerife, Spain

<sup>2</sup> Departamento de Astrofísica, Universidad de La Laguna, Tenerife, Spain

<sup>3</sup> Instituto Nacional de Astrofísica, Óptica y Electrónica, Tonantzintla, Puebla, Mexico

<sup>4</sup> Institute of Astronomy, University of Cambridge, Cambridge, UK

<sup>5</sup> Departamento de Física - CFM - Universidade Federal de Santa Catarina, PO Box 476, 88040-900, Florianópolis, SC, Brazil

class characterization represents a significant part of the paper, that are discussed in detail as an illustration of the procedure. As we stress above, our qualitative analysis may have several other applications, e.g., (1) to gain physical insight when interpreting quantitative Star Formation Histories (SFHs) derived from modern automated tools, (2) for quick-look galaxy classification (not only in the local universe, but also at moderate-high redshifts, since the Hubble expansion shifts the UV-visible spectrum to the near IR), (3) for interpreting noisy spectra where eyeball inspection is often better than detailed inversion, (4) as reference for identifying unusual galaxies, or (5) for educational purposes to develop physical intuition.

The paper is organized as follows. Section 2 introduces the ASK spectral classification of galaxy spectra whose templates serve as reference point. Section 3.1 lists and discusses spectral features commonly used when interpreting galaxy spectra. They are employed to set up the recipe introduced in Sect. 3.2, which is abridged in a schematic shown in Fig. 11. The recipe (or algorithm) is used in Sect. 4 to disclose the physical properties of all the ASK classes. The results of such qualitative analysis are compared with state-of-the-art quantitative analyses in Sects. 5 and 6 – Sect. 5 deals with the comparison of stellar components, whereas Sect. 6 refers to the gas components. Section 7 discusses several additional properties of the ASK templates, whereas Sect. 8 summarizes the proposed qualitative analysis.

## 2. ASK CLASSIFICATION

Sánchez Almeida et al. (2010) classified all the galaxies with spectra in SDSS-DR7 into only 28 ASK classes. The original SDSS covers one-fourth of the sky and contains the spectra of all the galaxies above an apparent magnitude threshold (SDSS  $r < 17.8$ ). Therefore, the some one million SDSS spectra can be regarded as representative of the galaxies of the local universe, and so do the ASK classes inferred from them. The ASK classification is detailed in Sánchez Almeida et al. (2010), with additional properties of the classes discussed elsewhere (Sánchez Almeida et al. 2011; Ascasibar & Sánchez Almeida 2011; Aguerri et al. 2012). For the sake of comprehensiveness, however, we summarize here the main properties. All galaxies with redshift smaller than 0.25 were transformed to a common rest-frame wavelength scale, and then re-normalized to the integrated flux in the SDSS  $g$ -filter. These two are the only manipulations the spectra underwent before classification. We wanted the classification to be driven only by the shape of the visible spectrum (from 400 to 770 nm), and these two corrections remove obvious undesired dependencies of the observed spectra on redshift and galaxy apparent magnitude. We deliberately avoided correcting for other effects requiring modeling and assumptions (e.g., dust extinction, seeing, or aperture effects). The employed classification algorithm, k-means, is a robust workhorse that allows the simultaneous classification of the full data set ( $\sim 12$  GB). It is commonly employed in data mining, machine learning, and artificial intelligence (e.g., Everitt 1995; Bishop 2006), and it guarantees that similar rest-frame spectra belong to the same class. Most galaxies (99%) were assigned to only 17 major classes, with 11 additional

minor classes including the remaining 1%. It is unclear whether the ASK classes represent genuine clusters in the 1637-dimensional classification space, or if they slice a continuous distribution – probably the two kinds of classes are present (see Sánchez Almeida et al. 2010; Ascasibar & Sánchez Almeida 2011).

All the galaxies in a class have very similar spectra, which are also similar to the class template spectrum formed as the average of all the spectra of the galaxies in the class. These template spectra are the ones analyzed in the paper. The averaging is slightly different from the one in Sánchez Almeida et al. (2010), and the novelty allows us to reach the near UV of the spectrum. The SDSS spectrograph detects from 3800 Å to 9200 Å (e.g., Stoughton et al. 2002), however, the templates cover from 3000 Å to 9200 Å. The UV extension is recovered because the classified galaxies have redshifts up to 0.25, which moves the rest-frame  $\lambda 3000$  Å within the observed range. Rather than averaging the spectral range common to all galaxies, the new templates consider the full range of available rest-frame wavelengths. Given a wavelength bin, it includes the spectra of all the galaxies in the class that have been observed at that particular rest-frame wavelength. Consequently, the template spectra (i.e., the average spectra) include wavelengths down to 3000 Å. The templates thus obtained vary smoothly and continuously. They are labeled according to the  $u - g$  color, from the reddest, ASK 0, to the bluest, ASK 27. The use of numbers to label the classes does not implicitly assumes the spectra to follow a one dimensional family. The numbers only name the classes. The sorting (and, so, the naming) would have been slightly different using other bandpasses to define colors. In general, however, the smaller the ASK class number the redder the spectrum. The ASK classification of all galaxies with spectra in SDSS-DR7 is publicly available, templates included<sup>6</sup>. Wavelengths of SDSS spectra (and of ASK templates) are vacuum wavelengths. However, all the spectra shown in this paper are transformed to air wavelengths according to the equations by Ciddor (1996). The SDSS spectra used for classification, and so the templates shown along the paper, are given as flux per unit wavelength.

## 3. RECIPE FOR QUALITATIVE INTERPRETATION OF GALAXY SPECTRA

Galaxies have composite spectra. They integrate contributions from different stars of different stellar populations, from HII regions, from Active Galactic Nuclei (AGNs), as well as from other possible components (e.g., hydrogen ionized by old high temperature stars, or by the intergalactic UV background – Cid Fernandes et al. 2004, 2010). Our qualitative analysis builds on this fact, and tries to separate each spectrum into a minimum number of components. We consider the (ionized) gas and the stars separately, that is to say, the emission and absorption lines separately. Each one of these two components is assumed to have one or two sub-components. The details on the characterization are summarized as

<sup>6</sup> [ftp://ask.galaxy@ftp.iac.es/](http://ask.galaxy@ftp.iac.es/)  
<http://sdc.cab.inta-csic.es/ask/index.jsp> in the Spanish Virtual Observatory.

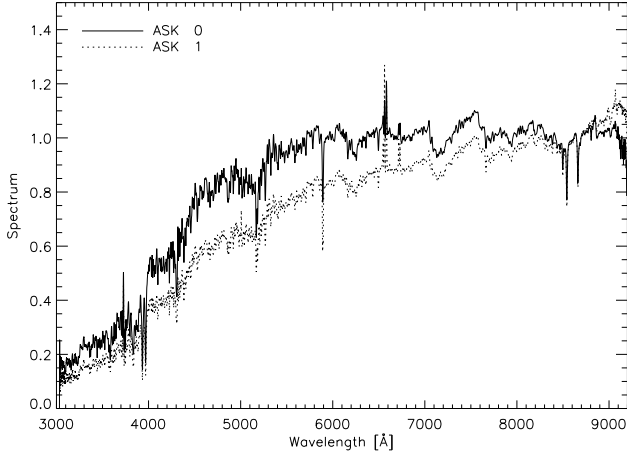


FIG. 1.— Effect of dust in the continuum. ASK 0 is the prototype of galaxy with red stellar populations. Since ASK 1 is even redder (i.e., the continuum has larger slope), its continuum must be affected by significant extinction. The presence of strong emission lines in ASK 1 reinforces the conclusion. The spectra are given as flux per unit wavelength, here and throughout the paper.

a decision tree in Sect. 3.2. It is based on the analysis of a set of general spectral features, listed in the next sub-section.

### 3.1. Spectral features to be considered in a qualitative analysis

The main spectral features that can be considered are listed in the section, ordered from the more obvious to the subtle details. Each item names the particular feature, and then outlines its main properties and interest. The actual features are illustrated using the appropriate ASK templates.

1. The shape of the continuum and the presence or not of emission and absorption lines must be considered. The emission lines trace the ionized gas and its excitation mechanism. The absorption lines trace the stellar populations, their ages and metallicities. The overall continuum shape is modulated by the gas, the stars, as well as by the presence of dust. Figure 1 shows the prototype red galaxy with passively evolving stellar populations (ASK 0). Although red, the continuum is rather flat from 6000 Å on. Spectra even redder must be shaped by dust extinction (see ASK 1 in Fig. 1).
2. The so-called 4000 Å *break* is produced by the absorption of metallic lines of a variety of elements in various states of ionization, including Ca II H and K ( $\lambda\lambda$  3969 Å and 3934 Å) and high-order lines of the Balmer series (H $\epsilon$   $\lambda$  3970 Å, H $\zeta$   $\lambda$  3889 Å, H $\eta$   $\lambda$  3835 Å, ...) (see Hamilton 1985, and also Fig. 2). The opacity suddenly increases for photons bluer than this wavelength, which produces an intensity drop. It is enhanced in old stellar populations (ASK 0), which tend to be metal rich, but it is also present in younger galaxies (ASK 19 in Fig. 2). The Balmer lines become deeper and broader with time from the starburst, with a characteristic time-scale of the order of one Gyr (e.g.,

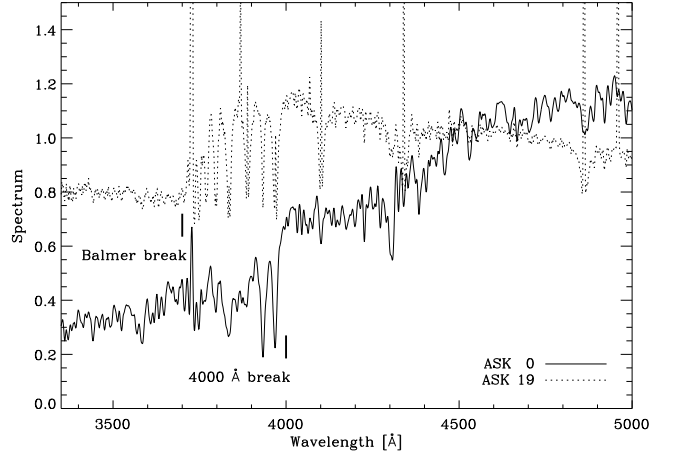


FIG. 2.— Spectra showing the 4000 Å break, as well as the break produced by the Balmer limit at 3650 Å.

González Delgado et al. 1999).

3. The limit of the Balmer series and the blending of the high-order Balmer lines also produces a notable discontinuity of the spectrum blueward of 3650 Å. It is the *Balmer break* – see Fig. 2. (Photons bluer than this limit ionize the excited hydrogen, thus H becomes an important source of continuum opacity.) It is present in young and old stellar populations, but it is more important in the young populations where H is a major constituent of the opacity (especially in the Balmer continuum beyond the discontinuity). The break amplitude and position is a proxy for the age of the stellar population (e.g., Aretxaga et al. 2001).
4. The Ca II H and K lines ( $\lambda\lambda$  3969 Å and 3934 Å, respectively) are typical of old metal-rich stars. Ca II H is blended with H $\epsilon$  which, as the rest of the Balmer series, appears in absorption in young stars (say, A stars). In case of mixed populations of old and young stars, the relative intensities of Ca II H and Ca II K (actually, of Ca II K and Ca II H+H $\epsilon$ ) is a proxy for the relative importance of the young and old populations. When Ca II K is larger than Ca II H, then the old population dominates the spectrum (ASK 2 in Fig. 3). As the young population becomes more important then Ca II H becomes stronger than Ca II K (ASK 9 in Fig 3). The relative growth reverts when the H II regions accompanying the young stellar populations produce enough H $\epsilon$  emission, which fills the Ca II H+H $\epsilon$  absorption profile (ASK 14 in Fig 3).
5. The UV continuum flux is also an age indicator for very young stellar populations. It increases with decreasing age when the ages are only a few Myr – see Fig. 4 and, e.g., Mas-Hesse & Kunth (1999). A symptom of extreme youth is the Balmer continuum showing up in emission ( $\lambda < 3650$  Å), as it happens with ASK 25 in Fig. 4.
6. The ratio between the fluxes of H $\alpha$  and [NII]  $\lambda$  6583 is an indicator of whether the nebula is ionized by

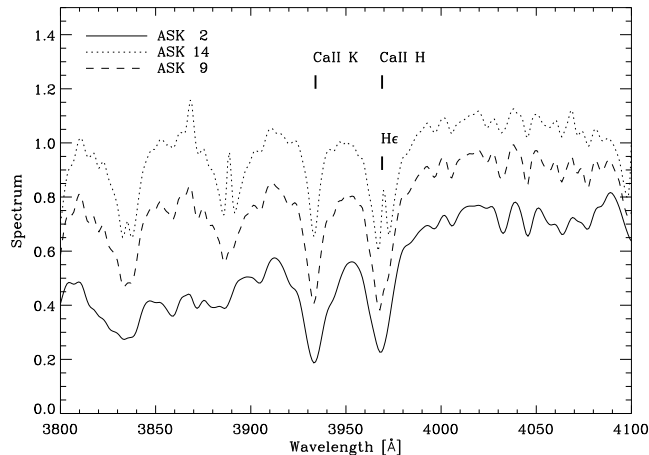


FIG. 3.— Spectra in the range of the Ca II H and K lines. Ca II H is blended with He. In case of mixed young and old stellar populations, the relative importance of Ca II K and the blended Ca II H informs on the relative importance of the two populations. Ca II K dominates in old populations (ASK 2), and Ca II H dominates when the young stars are more important (ASK 9), but the relationship saturates when He starts to show up in emission (ASK 14).

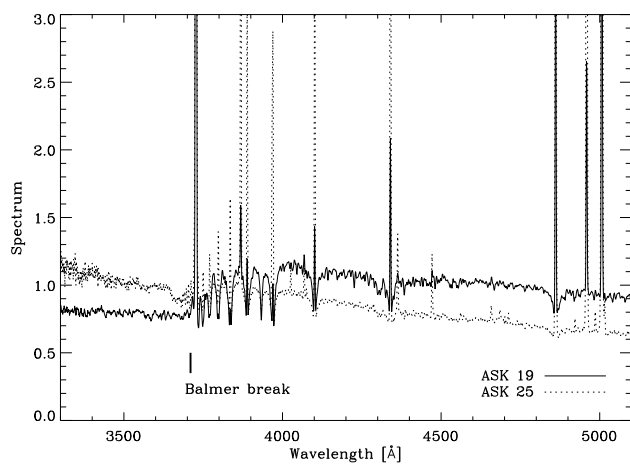


FIG. 4.— Spectra showing the increase of the UV continuum to the blue of 3650 Å as the stellar populations become younger (from ASK 19 to ASK 25).

a starburst ( $H\alpha \gg [NII]\lambda 6853$ ), or by a source of harder UV flux like an AGN or low mass evolved stars ( $H\alpha/2.5 \leq [NII]\lambda 6853$ ). Figure 5 shows examples of the two possibilities: a starburst (ASK 9) and a LINER-like excitation<sup>7</sup> (ASK 0). Once the ratio  $[NII]\lambda 6853$  to  $H\alpha$  is observed to be outside the starburst regime, Seyferts and LINERs can be distinguished according to the ratio of fluxes between  $[OIII]\lambda 5007$  and  $H\beta$  (Fig. 6) – the high ionization source is a Seyfert if  $[OIII]\lambda 5007 \gg H\beta$  (ASK 6) or

<sup>7</sup> We use the term *LINER-like* to refer to real Low-ionization nuclear emission-line regions (Heckman 1980), or evolved stars in retired galaxies (Flores-Fajardo et al. 2011), or X-ray emitting gas (e.g., Yan & Blanton 2012), or any other source with an ionizing UV spectrum harder than that of newborn stars, but not as hard as in a Seyfert galaxy or a quasar. Shock heated gas may also produce lines in this part of the diagram (e.g., Baldwin et al. 1981; Allen et al. 2008).

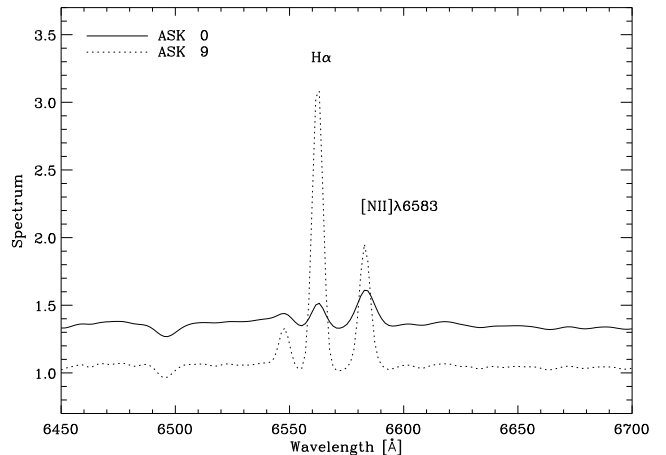


FIG. 5.— The ratio between  $H\alpha$  and  $[NII]\lambda 6853$  indicates whether the nebula is ionized by a starburst, or by other type of source with higher ionization power (e.g., AGNs).  $H\alpha \gg [NII]\lambda 6853$  indicates starburst (ASK 9) whereas  $[NII]\lambda 6853 \geq H\alpha$  is a symptom of higher ionization (ASK 0).

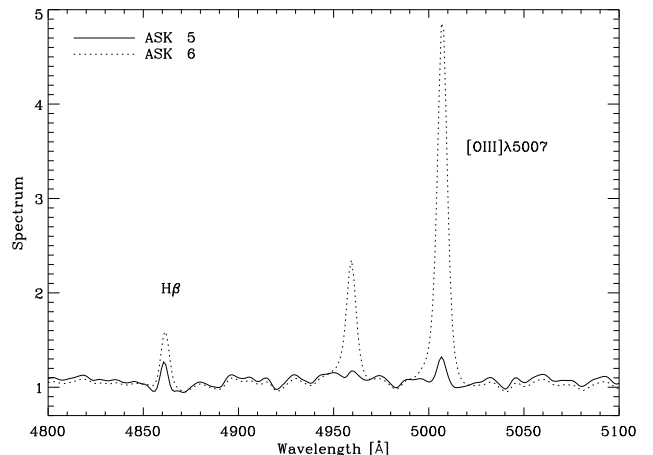


FIG. 6.— After establishing that the galaxy is not a starburst, the ratio between  $H\beta$  and  $[OIII]\lambda 5007$  indicates whether the ionization is powered by a strong AGN ( $[OIII]\lambda 5007 \gg H\beta$  – ASK 6) or by a LINER-like source ( $[OIII]\lambda 5007 \lesssim H\beta$  – ASK 5).

LINER-like if  $[OIII]\lambda 5007 \lesssim H\beta$  (ASK 5). This recipe is a qualitative rendering of the so-called BPT diagram (Baldwin et al. 1981) and its updates (Kauffmann et al. 2003; Kewley et al. 2006; Cid Fernandes et al. 2010).

7. The ratio between the fluxes of  $[NII]\lambda 6853$  and  $H\alpha$  also provides an estimate of gas metallicity in star-forming galaxies (Denicoló et al. 2002). The sensitivity is high: the ratio goes from 1/3 to 1/300 when the metallicity ranges from solar to one tenth solar (Pettini & Pagel 2004). This high contrast makes it simple to distinguish between solar and sub-solar metallicities. The ratio is not suitable to diagnose super-solar metallicities. In this case one can use supplementary line ratios like the so-called R23 or O3N2 (e.g., Alloin et al. 1979; Pagel et al. 1979; Shi et al. 2005).

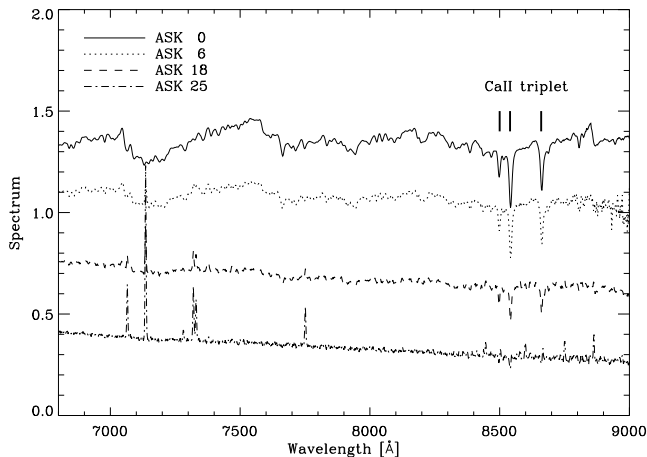


FIG. 7.— The TiO bands at approximately 7150 Å, 7600 Å, and 8500 Å are characteristic of M stars, and they appear in all ASK classes except for the bluest ones (ASK 25 in the plot). Note also the presence of the IR Ca II triplet in the middle of the third TiO band ( $\lambda\lambda 8498, 8542$ , and  $8662$  Å).

8. The presence of [OIII] $\lambda 4363$  is also an indicator of low metallicity. The line is used to compute electron temperatures in HII regions, and it weakens with increasing metallicity to disappear at around  $12 + \log(\text{O}/\text{H}) \gtrsim 8.2$  (e.g., McGaugh 1991).
9. TiO bands at approximately 7150 Å, 7600 Å, and 8500 Å are characteristic of M stars (dwarf, giant and super-giants; e.g., Allard et al. 2000), and reveal the presence of evolved stellar populations. When the stellar population is young, massive stars outshine the contribution of M stars, making these spectral features invisible. (Red super-giants are young massive stars showing TiO bands, but they are outnumbered by the associated blue super-giants that overshadow their contribution to the integrated galaxy spectrum – e.g., Maeder et al. 1980; Massey 2002.) Figure 7 shows how the TiO bands appear in almost all ASK classes, except for the bluest ones, and how the strength of the bands decrease as the spectrum becomes bluer. As we mention in Sect. 4, the bands are hardly noticeable at ASK 16, and they are absent at ASK 20 and bluer types.
10. The IR Ca II triplet at  $\lambda\lambda 8498, 8542$ , and  $8662$  Å is an indicator of metallicity and gravity. In stars, its equivalent width (EW) increases with increasing metallicity until  $2/3$  of the solar metallicity (Diaz et al. 1989). Above this metallicity it depends only on gravity, with the EW increasing with decreasing gravity from dwarfs to super-giants (Diaz et al. 1989; Cenarro et al. 2002). The combined effect on galaxy spectra must be modeled, but the existence of a Ca II absorption with significant strength is always a sign of high metallicity and of the presence of giant stars. Contrarily, absence of the triplet indicates low metallicity. We find it in all ASK spectra except for the bluest classes (see Fig. 7). As we mention in Sect. 4, the lines are almost absent in ASK 20 and bluer

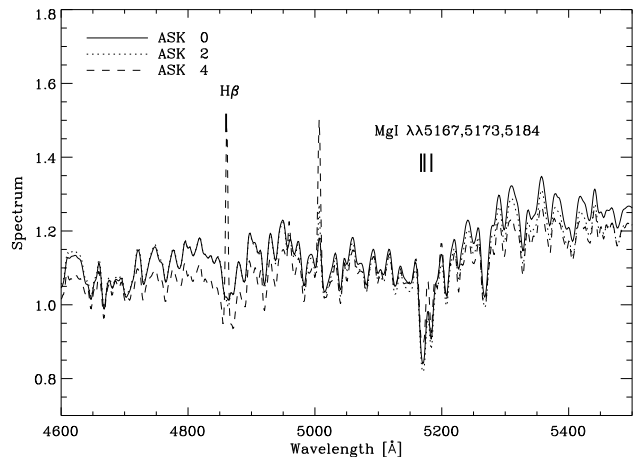


FIG. 8.— Spectral region containing the spectral indices  $H\beta$  and  $Mg_2$  ( $H\beta$  index from 4848 to 4877 Å, and  $Mg_2$  from 5154 to 5197 Å). Both indices combined allow us to set mean age and mean metallicity in galaxies with old stellar populations. The labels mark the  $H\beta$  line and the position of the three Mg I lines contributing to  $Mg_2$ .

classes.

11. The so-called  $Mg_2$  and  $H\beta$  Lick indices are in the same spectral region ( $H\beta$  from 4848 to 4877 Å, and  $Mg_2$  from 5154 to 5197 Å; see Fig. 8), and they were designed (and are used) to determine simultaneously age and metallicity in galaxies with old stellar populations (Worthey et al. 1994). One can generally say that  $H\beta$  mostly depends on age, and to less extent on metallicity, and the opposite happens with  $Mg_2$  (e.g., Vazdekis et al. 1996; Jørgensen 1999). However, their quantitative application require modeling (e.g., they may depend on the relative abundance of the metals, rather than on a single global metallicity).
12. The interstellar medium (ISM) that reddens the spectra also produces absorption in the Na I D line ( $\lambda\lambda 5891, 5896$  Å, e.g., Asari et al. 2007; Chen et al. 2010). Therefore, one would expect that the strength of the ISM Na I D line sorts galaxies according to extinction (Asari et al. 2007). The example in Fig. 9 corresponds to the two spectra in Fig. 1, where ASK 1 is known to present a substantial dust extinction. Its Na I D is stronger than that for the class without extinction, ASK 0, being the rest of the spectrum similar.
13. The mere presence of high excitation lines like [Ne V] $\lambda 3426$ , [Fe VII] $\lambda 6087$ , or [Fe X] $\lambda 6375$ , tells us that the galaxy hosts an AGN (e.g., Reunanen et al. 2003; Goulding & Alexander 2009; Rodríguez-Ardila et al. 2011). The example in Fig. 10 shows spectra in the range of [Fe VII] $\lambda 6087$ , whose emission is clear in Seyferts (ASK 7 and 8), but is non-existing in starbursts (ASK 20) as well as in passively evolving red galaxies with LINER-like emission (ASK 0; see Sect. 4). [He II] $\lambda 6686$  is also indicative of AGN, though it is sometimes found in star forming galaxies (e.g., Schaerer et al.

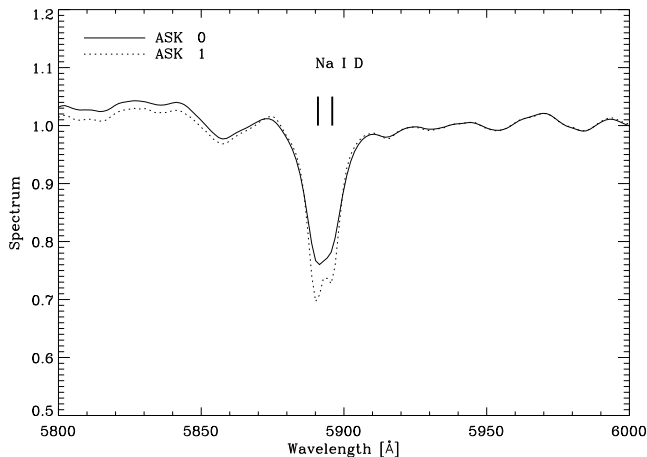


FIG. 9.— Na I D is partly produced by ISM absorption. It is larger for the class with larger dust extinction (c.f., Fig. 1).

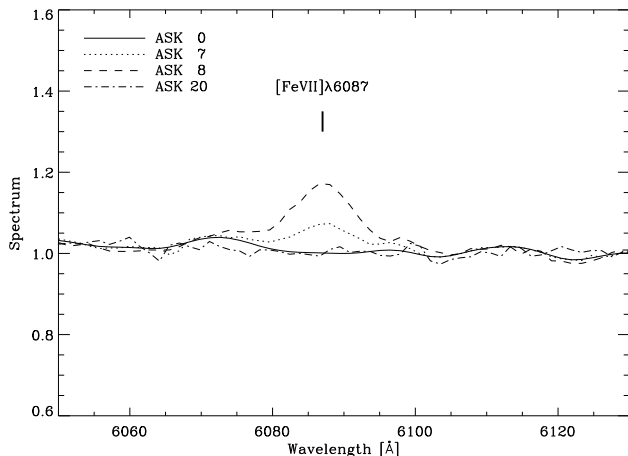


FIG. 10.— Spectral range containing the high excitation line [FeVII] $\lambda$ 6087, clear in Seyferts (ASK 7 and 8) but non-existing otherwise. (ASK 20 is a starbursts, whereas ASK 0 represents a passively evolving red galaxy.)

1999; Shirazi & Brinchmann 2012).

### 3.2. Decision tree for qualitative analysis of galaxy spectra

Considering the spectral features described in the previous section, we have set up a simple decision tree (a questionnaire) that leads to classifying a galaxy spectrum by replying to a few questions (Fig. 11). Emission and absorption lines are analyzed separately, therefore, the natural outcome would be galaxy types with two components, one for the stars and other for the gas. One should begin the questionnaire from top to bottom, to end up with the characteristics of both the gas and the stars.

The decision tree in Fig. 11 is self-explanatory, although a few clarifications on the terminology are required. The symbol G stands for galaxy. *Broad spectral lines* means lines in excess of  $2000 \text{ km s}^{-1}$ , and they separate Seyfert 1 and quasars from the other kinds of AGNs. Such broad lines are not illustrated in Sect. 3.1 since the ASK classes lack Seyfert 1 and quasars, that were excluded from the list of galaxy targets directly at

the SDSS distribution (see Schneider et al. 2007). When we mention young, old and a mixture of old-and-young stellar populations, we loosely speaking refer to stellar ages  $< 10^7$  yr (young),  $> 10^9$  yr (old), and the intermediate range in between,  $10^7$ – $10^9$  yr. When metal poor gas is mentioned, we mean clearly sub-solar (say, less than  $1/3$  solar). BL Lac objects are also included to complete the questionnaire, so that it considers the possibility that neither emission nor absorption lines are present in the spectrum (Stein et al. 1976; Massaro et al. 2012). Several criteria in Fig. 11 compare emission lines – such comparison refers to the fluxes of the lines.

## 4. QUALITATIVE ANALYSIS OF THE ASK CLASSES

One may think of this section as analogous to the section on *individual objects*, common in many papers, except that the targets are ASK templates representing objects too numerous to be described one by one. We use the criteria put forward in the previous section to determine the properties of all ASK classes individually. The thread of the argumentation follows the decision tree in Fig. 11. A summary with the properties of all classes is also given in Table 1. At the end of the section, we define a stellar age index that sorts the ASK classes according to their mean stellar age. Similarly, we define an index to sort the emission line spectra by metallicity. Both are relative quantities, devised to compare our qualitative analysis with quantitative estimates of ages and metallicities.

- ASK 0 has an absorption line spectrum with very weak emission lines (Fig. 1). It is not a starburst since  $[\text{NII}]\lambda 6853 > \text{H}\alpha$ , but  $[\text{OIII}]\lambda 5007$  and  $\text{H}\beta$  are too weak to decide whether the excitation is Seyfert-like or LINER-like. Note, however, that the EW of  $\text{H}\alpha$  is very small (Fig. 5), which according to Cid Fernandes et al. (2011) indicates that the ionization is produced by hot-low mass stars. The absorption line spectrum does not show the Balmer break (Fig. 2) but the  $4000 \text{ \AA}$  break is conspicuous, consequently, the absorption spectrum is produced by an old metal-rich stellar population.

- ASK 1 also has an absorption line spectrum with weak emission lines (Fig. 1).  $[\text{NII}]\lambda 6853 \simeq \text{H}\alpha$ , and therefore it is not a starburst.  $\text{H}\beta$  is smaller than  $[\text{OIII}]\lambda 5007$ , which may naively indicate AGN excitation. However, the lines are so weak that the underlying  $\text{H}\beta$  absorption is important and, therefore the corrected  $\text{H}\beta$  emission is similar to that of  $[\text{OIII}]\lambda 5007$ . Consequently, the emission line spectrum is probably in the LINER region of the BPT diagram. The absorption line spectrum is also very similar to ASK 0, which was assigned to an old metal-rich stellar population. The main difference with respect to ASK 0 is the continuum, which steepens redward of  $6000 \text{ \AA}$  (Fig. 1), and is a signature of dust reddening. Additional independent arguments also corroborate that ASK 1 owes much of its red colors to reddening. ASK 1 galaxies tend to have very elongated morphologies, a fact difficult to interpret unless they are edge-on disks (Sánchez Almeida et al. 2011), which are known to be significantly dust reddened with respect to their face-on counterparts (e.g., Giovanelli et al. 1994; Masters et al. 2010).

- ASK 2 is very similar to ASK 0, so does our assign-

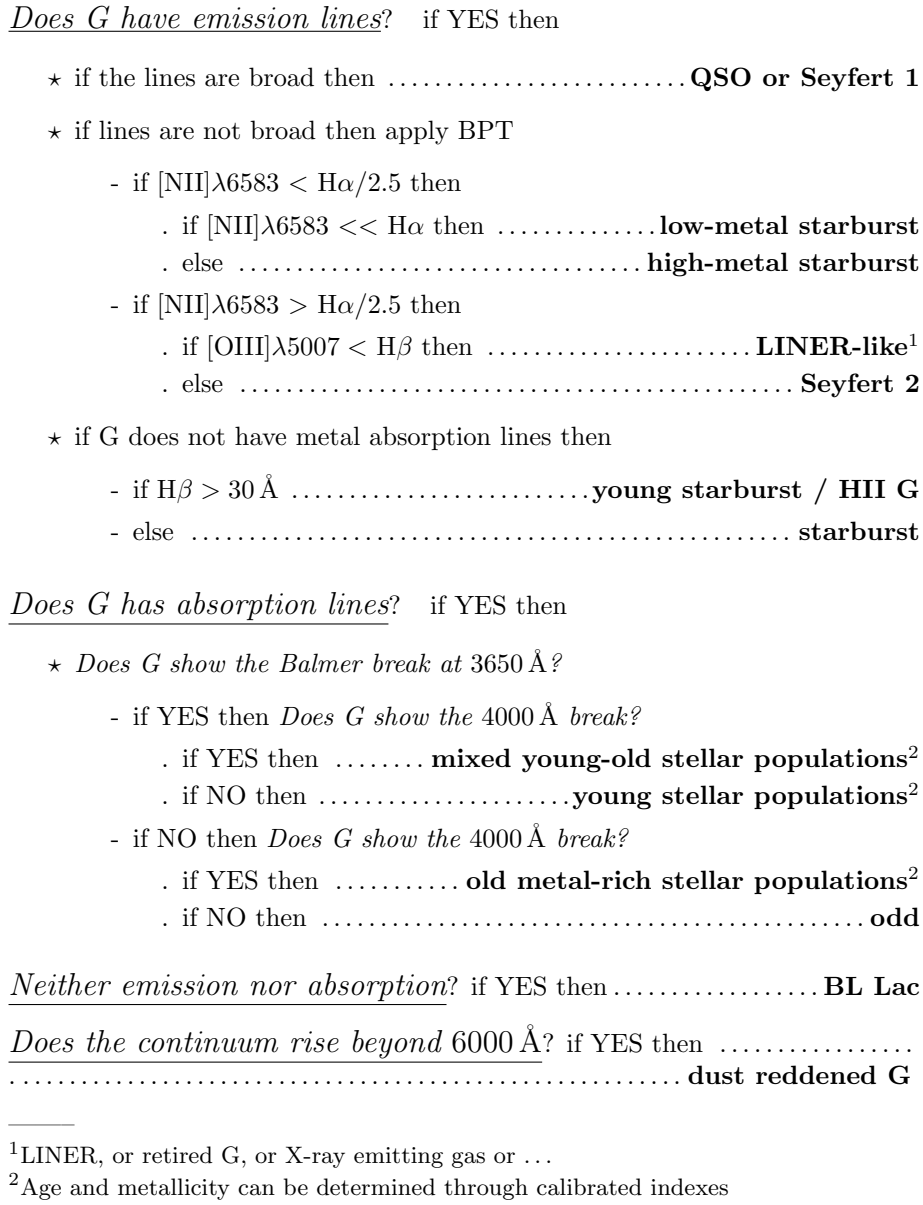


FIG. 11.— Decision tree for qualitative classification of galaxy spectra. The questions to be replied are written in italic fonts. The galaxy types resulting from the analysis are written in bold fonts on the right hand side of the panel. The symbol G stands for galaxy. See Sect. 3.2 for further details.

nation – emission consistent with AGN or LINER-like excitation plus absorption corresponding to old metal-poor stars. The difference is in the continuum, which is somewhat redder in ASK 0, and also in the emission line [SIII] $\lambda$ 9069, which shows up in ASK 2 but not in ASK 0.

- ASK 3 also shows an absorption line spectrum with weak emission. Emissions and absorptions are similar to those of ASK 0, therefore, the associated stellar population is old. As it happens with ASK 0, [OIII] $\lambda$ 5007 and  $H\beta$  are too weak to decipher whether the emission is Seyfert or LINER-like. The difference with ASK 0, 1 and 2 is the continuum, which is bluest in ASK 3 (see Fig. 12). Except for ASK 1, such variation reflects differences in the stellar populations, ASK 3 being the

youngest. ASK 0, 2, and 3 were used to select a clean sample of red ellipticals by Aguerri et al. (2012).

- ASK 4 spectrum has absorption lines and significant emission lines. The continuum is fairly red, similar to that of ASK 0 in Fig. 1.  $H\alpha \simeq 2 \times [\text{NII}]\lambda 6853$  and  $H\beta \gtrsim [\text{OIII}]\lambda 5007$ , therefore, according to the decision tree (Fig. 11), it should be a LINER-like galaxy. However, it is in the region of the BPT diagram where AGN activity and star-formation are difficult to disentangle (see Fig. 13 in Sánchez Almeida et al. 2010). The absorption line spectrum shows both the Balmer break and the 4000  $\text{\AA}$  break, which correspond to a mixture of old and young stellar populations. The region around the

TABLE 1  
QUALITATIVE PHYSICAL PROPERTIES OF THE ASK TEMPLATE SPECTRA

ASK class	emission (gas)	absorption (stars)	comment	SAI <sup>c</sup>	GMI <sup>d</sup>	O/H <sup>e</sup> (gas)	Age [Gyr] <sup>f</sup> (stars)	Z/Z <sub>⊙</sub> <sup>f</sup> (stars)
0	AGN or LINER-like	old metal-rich	H $\alpha$ EW $\simeq$ 0.9Å <sup>a</sup>	0	—	—	11.2 $\pm$ 1.2	1.30 $\pm$ 0.34
1	LINER-like	old metal-rich	dust reddened, edge on disks? <sup>b</sup>	0	—	—	10.0 $\pm$ 1.4	0.91 $\pm$ 0.34
2	AGN or LINER-like	old metal-rich	[SII] $\lambda$ 9069 emission	1	—	—	11.1 $\pm$ 1.2	1.31 $\pm$ 0.34
3	LINER-like	old metal-rich	continuum bluer than ASK 0 and 2	2	—	—	6.7 $\pm$ 1.2	1.57 $\pm$ 0.38
4	LINER-like?	old & young	edge-on disks? <sup>b</sup>	3	—	—	7.4 $\pm$ 1.5	0.69 $\pm$ 0.36
5	LINER-like?	old & young	green valley galaxies <sup>a</sup>	3	—	—	6.0 $\pm$ 1.4	1.21 $\pm$ 0.43
6	Seyfert 2	old & young	[FeVII] $\lambda$ 6087 emission	3	—	—	5.3 $\pm$ 1.3	1.35 $\pm$ 0.44
7	Seyfert 2	old & young	younger than 6, [FeVII] $\lambda$ 6087 emission	4	—	—	5.2 $\pm$ 1.2	1.23 $\pm$ 0.44
8	Seyfert 2	old & young	younger than 7, [FeVII] $\lambda$ 6087 emission	5	—	—	2.30 $\pm$ 0.71	1.05 $\pm$ 0.44
9	LINER-like	old & young	metal-rich starburst?	3	—	—	3.6 $\pm$ 1.2	1.01 $\pm$ 0.44
10	metal-rich starburst	old & young	LINER-like?	3	-0.35	—	4.1 $\pm$ 1.3	0.61 $\pm$ 0.34
11	metal-rich starburst	old & young	LINER-like?, stars younger than 9 and 10	4	-0.36	—	4.8 $\pm$ 1.4	0.43 $\pm$ 0.24
12	metal-rich starburst	old & young	starburst prototype, stars younger than 11	6	-0.43	8.46 $\pm$ 0.18	2.7 $\pm$ 1.1	0.68 $\pm$ 0.35
13	metal-rich starburst	old & young	stars similar to 12	6	-0.46	—	2.30 $\pm$ 0.93	0.90 $\pm$ 0.41
14	metal-rich starburst	old & young	starburst prototype, stars younger than 12	7	-0.46	8.50 $\pm$ 0.11	1.71 $\pm$ 0.92	0.60 $\pm$ 0.30
15	metal-poor starburst	no absorption	HII G, youngest ASK	—	-1.67	7.85 $\pm$ 0.05	—	—
16	metal-poor starburst	old & young	—	7	-0.63	8.77 $\pm$ 0.10	1.18 $\pm$ 0.72	0.58 $\pm$ 0.30
17	metal-poor starburst	young	HII G, stars older than 15	13	-1.58	8.06 $\pm$ 0.02	0.0048 $\pm$ 0.0008	1.29 $\pm$ 0.43
18	metal-poor starburst	young	stars younger than 16	8	-0.54	8.61 $\pm$ 0.04	0.090 $\pm$ 0.038	0.52 $\pm$ 0.24
19	metal-poor starburst	young	stars as in 18	8	-0.75	8.72 $\pm$ 0.05	0.249 $\pm$ 0.077	0.51 $\pm$ 0.25
20	metal-poor starburst	young	HII G, stars younger than 18, older than 17	13	-1.42	8.19 $\pm$ 0.01	0.0045 $\pm$ 0.0007	0.60 $\pm$ 0.33
21	metal-poor starburst	young	HII G, like 20, gas slightly metal-poorer	13	-1.45	8.07 $\pm$ 0.01	0.0073 $\pm$ 0.0019	0.72 $\pm$ 0.34
22	metal-poor starburst	young	like 19, stars younger, gas metal-richer	8	-0.93	8.59 $\pm$ 0.04	0.138 $\pm$ 0.057	0.39 $\pm$ 0.17
23	metal-poor starburst	young	like 19 and 22, stars younger	9	-0.79	8.60 $\pm$ 0.02	0.056 $\pm$ 0.031	0.45 $\pm$ 0.24
24	metal-poor starburst	young	like 23, stars younger	10	-1.07	8.48 $\pm$ 0.02	0.062 $\pm$ 0.035	0.44 $\pm$ 0.22
25	metal-poor starburst	young	like 20 and 21, stars older, gas metal-richer	12	-1.27	8.29 $\pm$ 0.01	0.0083 $\pm$ 0.0018	0.72 $\pm$ 0.36
26	metal-poor starburst	young	like 25, stars older, gas metal-richer	11	-1.09	8.38 $\pm$ 0.02	0.0090 $\pm$ 0.0020	0.49 $\pm$ 0.28
27	metal-poor starburst	young	like 25	12	-1.18	8.23 $\pm$ 0.02	0.0098 $\pm$ 0.0033	0.71 $\pm$ 0.34

<sup>a</sup> From Sánchez Almeida et al. (2010), Table 2.

<sup>b</sup> Sánchez Almeida et al. (2011).

<sup>c</sup> Stellar Age Index, which orders stellar ages starting from the oldest (SAI=0)

<sup>d</sup> Gas Metallicity Index ( $\equiv \log([NII]\lambda 6853/H\alpha)$ ), which orders galaxies according to gas metallicity.

<sup>e</sup>  $12 + \log(O/H)$  obtained via electron temperature and density. The error bars account for uncertainties inherited from errors in line fluxes.

<sup>f</sup> Luminosity-weighted average values using STARLIGHT. The error bars represent the dispersion among the SSP that contribute to the integrated light.

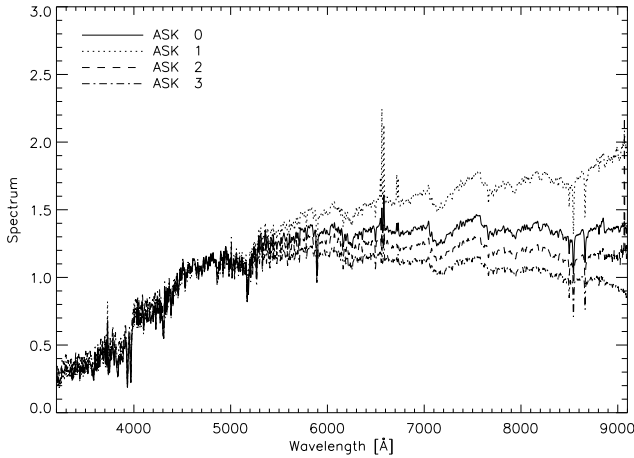


FIG. 12.— Full spectral range for ASK 0, 1, 2, and 3 as indicated. The absorption features are similar but the continua become redder as the ASK number increases. This change is due to the aging of the stellar populations, except for ASK 1, which reflects enhanced extinction.

break is shown in Fig. 13.

• ASK 5 has absorption and emission lines. The continuum is significantly bluer than that for ASK 4.  $H\alpha \simeq 2 \times [NII]\lambda 6853$  and  $H\beta \gtrsim [OIII]\lambda 5007$ , therefore, according to the decision tree (Fig. 11), it should be a LINER-like galaxy (with the caveat issued for ASK 4 still

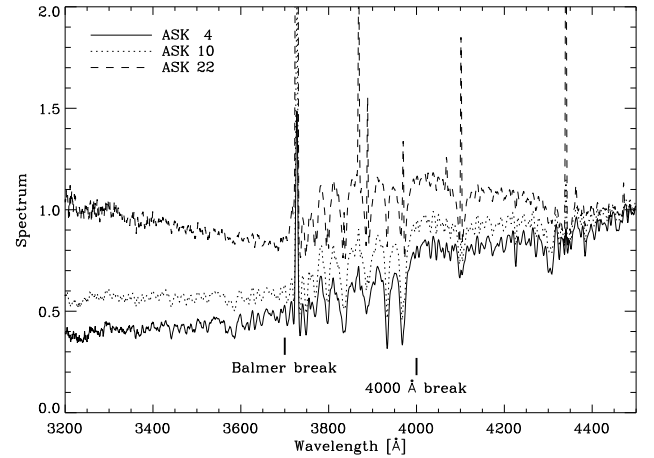


FIG. 13.— Gradual variation of the breaks at 3650 Å and 4000 Å that show the evolution from ASK 4 to ASK 22. ASK 4 has the oldest stellar population in the series. The 4000 Å break of ASK 4 is more intense than the Balmer break. Both are similar in ASK 10, and the 4000 Å break has disappeared in the case of ASK 22.

applying). The absorption line spectrum shows both the Balmer break at 3650 Å and the 4000 Å break, which correspond to a mixture of old and young stellar populations (like ASK 4 in Fig. 13).

• ASK 6 has intense emission lines on top of an absorp-

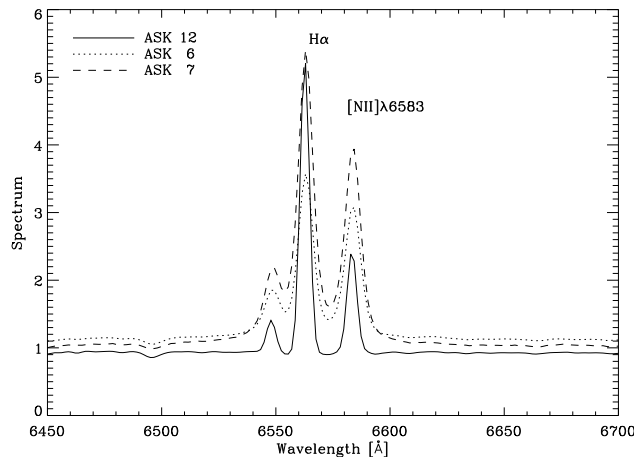


FIG. 14.— Line width differences between Seyfert galaxies with broad lines (ASK 6 and ASK 7), and starburst galaxies with narrow lines (ASK 12). Even if broad, the lines of ASK 6 and ASK 7 are not broad enough to be regarded as Seyfert 1.

tion spectrum. Emission lines are broad (Fig. 14), but not broad enough to be a Seyfert 1 galaxy (larger than  $2000 \text{ km s}^{-1}$ ). It appears in the Seyfert region of the BPT diagram, therefore it is a Seyfert 2.  $[\text{FeVII}]\lambda 6087$  and  $[\text{NeV}]\lambda 3426$  show up in emission confirming the AGN nature of the emission. It shows the Balmer break at  $3650 \text{ Å}$  and the  $4000 \text{ Å}$  break, which correspond to a mixture of old and young stellar populations. The breaks are extremely similar to that of ASK 4 in Fig. 13.

- ASK 7 is similar to ASK 6. The emission lines are broad (Fig. 14), and it is also classified as Seyfert 2 according to the decision tree.  $[\text{FeVII}]\lambda 6087$  is detected, confirming the AGN nature of the emission (Fig. 10). The absorption spectrum has a clear  $4000 \text{ Å}$  break, and the Balmer break is present but less pronounced than in the case of ASK 6 because the Balmer continuum rises blueward of the Balmer break. The absorption spectrum is also produced by a mixture of old and young stars, but probably younger than for ASK 6.

- ASK 8 is similar to ASK 6 and 7, but the emission lines are even broader. It is also a Seyfert 2.  $[\text{FeVII}]\lambda 6087$  is detected, confirming the AGN nature of the emission (Fig. 10). Following the trend from ASK 6 to ASK 7, the absorption spectrum shows the two breaks (Balmer and  $4000 \text{ Å}$ ), but the Balmer continuum (blueward of  $3650 \text{ Å}$ ) is more intense. The spectrum is also produced by a mixture of old and young stars, but probably younger than for ASK 7.

- ASK 9 has absorption and emission lines. The lines are narrow, and  $H\alpha \simeq 2 \times [\text{NII}]\lambda 6853$  with  $H\beta \gtrsim [\text{OIII}]\lambda 5007$ . According with the decision tree it has LINER-like emission, although it is close to being classified as a metal-rich starburst. The absorption spectrum presents well defined Balmer and  $4000 \text{ Å}$  breaks, therefore, it is produced by a mixture of old and young stellar populations. The region of the breaks is similar to that of ASK 5.

- ASK 10 has absorption and emission lines. The continuum is similar to that of ASK 9 except that it becomes redder beyond  $7000 \text{ Å}$ .  $H\alpha \simeq 2.5 \times [\text{NII}]\lambda 6853$  with  $H\beta \sim 2 \times [\text{OIII}]\lambda 5007$ . According with the decision tree

it corresponds to a metal-rich starburst, although it is close to the divide with LINER-like emission. The absorption spectrum is almost identical to the spectrum of ASK 9 in the region of the Balmer and  $4000 \text{ Å}$  breaks, and it is produced by a mixture of old and young stellar populations.

- ASK 11 has both absorption and emission, but the emission lines are very intense. The red continuum is redder than in ASK 9 and 10, but the emission lines of ASK 11 are stronger.  $H\alpha \simeq 3 \times [\text{NII}]\lambda 6853$  with  $H\beta \sim 2 \times [\text{OIII}]\lambda 5007$ . It corresponds to a metal-rich starburst, although it is close to the border to present LINER-like emission. The absorption spectrum is almost identical to the spectrum of ASK 9 in the region of the Balmer and  $4000 \text{ Å}$  breaks, except that the contribution of the Balmer lines is more important. It is produced by a mixture of old and young stellar populations, but the young population is more important than in the case of ASK 9 and 10.

- ASK 12 spectrum has both absorption and emission lines. The continuum is bluer than that of ASK 10 and 11, but the emission lines are weaker.  $H\alpha \simeq 2.5 \times [\text{NII}]\lambda 6853$  with  $H\beta \sim 1.5 \times [\text{OIII}]\lambda 5007$ . It represents a typical metal-rich starburst – it is right on the head of the *seagull* of the local BPT diagram corresponding to prototypical starbursts. The absorption line spectrum has the Balmer and  $4000 \text{ Å}$  breaks, but the  $4000 \text{ Å}$  break is less pronounced than that in ASK 10 and 11, and the Balmer series more intense. The spectrum corresponds to mixed old and young stellar populations, but the young population is more important than in the case of ASK 9, 10, and 11.

- ASK 13 spectrum has both absorption and emission lines. The continuum is bluer than that of ASK 11 and 12, but the emission lines are weaker.  $H\alpha \simeq 3 \times [\text{NII}]\lambda 6853$  with  $H\beta \sim 2 \times [\text{OIII}]\lambda 5007$ . It is a starburst. The absorption line spectrum has the Balmer and  $4000 \text{ Å}$  breaks, and they are almost identical to those for ASK 12. The spectrum corresponds to mixed old and young stellar populations similar to ASK 12.

- ASK 14 spectrum has both absorption and emission lines. The continuum is bluer than that of ASK 12 and 13, and the emission lines more pronounced.  $H\alpha \simeq 3 \times [\text{NII}]\lambda 6853$  with  $H\beta \sim 1.5 \times [\text{OIII}]\lambda 5007$ . It corresponds to a typical metal-rich starburst. The absorption line spectrum has the Balmer and  $4000 \text{ Å}$  breaks, but the  $4000 \text{ Å}$  break is barely noticeable. The spectrum corresponds to mixed old and young stellar populations, but the young population is more important than in the case of ASK 12, and 13.

- ASK 15 is a pure emission line spectrum. The EW of  $H\beta$  is of the order  $200 \text{ Å}$  therefore, according the decision tree, it is an HII galaxy.  $H\alpha \gg [\text{NII}]\lambda 6853$  with  $H\beta \ll [\text{OIII}]\lambda 5007$ , which corresponds to a low-metallicity starburst. The spectrum shows neither the Balmer break nor the  $4000 \text{ Å}$  break (even more extreme than ASK 17 in Fig. 15). There are no metallic lines, and even the Balmer series shows no trace of absorption. This spectrum corresponds to the youngest stellar populations of the ASK series. ASK 15 has only 68 members (Sánchez Almeida et al. 2010), most of which look compact galaxies, like those described by Cardamone et al. (2009) and Amorín et al. (2010), but a few of them are

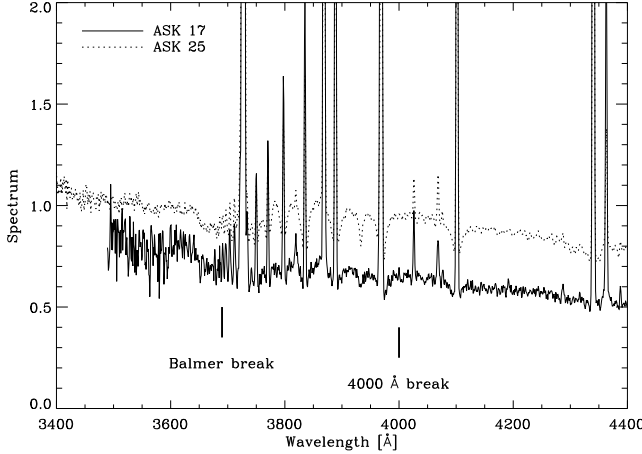


FIG. 15.— Spectra of HII galaxies. ASK 25 presents no 4000 Å break, but the Balmer break is clear, and the Balmer continuum appears in emission. The Balmer series shows both emission and absorption. ASK 17 represents a more extreme case where absorptions are almost absent, even those of the Balmer series. Note that the emission lines are well out-of-scale, with peaks of the order of 15 times the continuum.

HII regions in resolved galaxies.

- ASK 16 spectrum has both absorption and emission lines. The continuum is bluer than that of ASK 13 and 14 including the upturn at the UV.  $H\alpha \gg [NII]\lambda 6853$  with  $H\beta \sim [OIII]\lambda 5007$ , which corresponds to a metal-poor starburst. The absorption line spectrum does show the Balmer break, but the 4000 Å break is barely noticeable. Consequently, the absorption line spectrum corresponds to a young stellar population, with hints of an old component. The TiO bands are hardly noticeable.

- ASK 17 spectrum has only emission lines. (One can barely notice the absorption of some of the Balmer lines; see Fig. 15). Since the EW of  $H\beta \simeq 150$  Å, according to the decision tree ASK 17 is an HII galaxy. The continuum is as blue as that of ASK 15 and includes the UV upturn (Fig. 15).  $H\alpha \gg [NII]\lambda 6853$  with  $H\beta \ll [OIII]\lambda 5007$ , which corresponds to a metal-poor starburst. Even though absorption lines are not obvious, the spectrum shows the Balmer break (see Fig. 15). This two features correspond to extremely young stellar populations (although not as young as those involved in ASK 15).

- ASK 18 spectrum has absorption and strong emission lines. The continuum is similar to that of ASK 16 but the upturn of the UV continuum is more pronounced. The emission lines are also stronger than those of ASK 16.  $H\alpha \gg [NII]\lambda 6853$  with  $H\beta \simeq [OIII]\lambda 5007$ , which corresponds to a metal-poor starburst. The absorption line spectrum does show the Balmer break, but it does not have a 4000 Å break (similar to ASK 22 in Fig. 13). The absorption line spectrum corresponds to a young stellar population.

- ASK 19 spectrum presents absorption and strong emission lines. The continuum is bluer than that of ASK 18 but the emission lines are weaker.  $H\alpha \gg [NII]\lambda 6853$  with  $H\beta \ll [OIII]\lambda 5007$ , which corresponds to a metal-poor starburst. The absorption line spectrum shows the Balmer break, but it does not have a 4000 Å break, and it is similar to ASK 18. It corresponds to a

young stellar population.

- ASK 20 spectrum is dominated by strong emission lines but it also shows weak absorptions in the Balmer lines. The weak continuum is as blue as that of ASK 15, 17 or 19, and includes an UV upturn. We identify ASK 20 as an HII galaxy.  $H\alpha \gg [NII]\lambda 6853$  with  $H\beta \ll [OIII]\lambda 5007$ , which corresponds to a metal-poor starburst. The absorption line spectrum does show the Balmer break, but it does not have a 4000 Å break. It also contains metallic lines (Ca II H and K). The absorption line spectrum corresponds to a young stellar population. Stars are older than those in ASK 17, but younger than those in ASK 19. The TiO bands are absent, and the IR Ca triplet is almost gone with a hint of showing up in emission.

- ASK 21 is very similar to ASK 20, except that the lines are somewhat weaker. Probably the gas-phase metallicity is a bit higher in ASK 21 as judged from the ratio between  $H\alpha$  and  $[NII]\lambda 6853$ . In any case, the starburst is metal-poor.

- ASK 22 spectrum presents absorption and strong emission lines. The continuum is similar to ASK 19, but bluer. The emission lines are somewhat stronger than those in ASK 19.  $H\alpha \gg [NII]\lambda 6853$  with  $H\beta \ll [OIII]\lambda 5007$ , which corresponds to a metal-poor starburst. The gas metallicity is a bit higher in ASK 19, as judged from the ratio between  $H\alpha$  and  $[NII]\lambda 6853$ . The absorption line spectrum shows the Balmer break, but it does not have a 4000 Å break, and it is similar to ASK 19. The absorption line spectrum corresponds to a young stellar population, probably younger than that in ASK 19.

- ASK 23 spectrum is very similar to that of ASK 22 and ASK 19, except for having larger emission lines. The continuum is also a bit bluer. It corresponds to a metal-poor starburst with a young stellar population, presumably younger than that for ASK 19 and 22.

- ASK 24 has a spectrum similar to ASK 23 (and so to ASK 22 and 19), with stronger emission lines. The continuum is bluer than in ASK 23. As judged from the ratio between  $H\alpha$  and  $[NII]\lambda 6853$ , the gas metallicity of ASK 23 is higher.

- ASK 25 spectrum is similar to ASK 20 and 21, with the continuum a bit redder, and the lines weaker. As judged from the ratio between  $H\alpha$  and  $[NII]\lambda 6853$ , the gas metallicity of ASK 20 and 21 are smaller. The Balmer continuum shows up in emission (Fig. 15).

- ASK 26 spectrum is similar to ASK 25, with the continuum a bit redder, and the lines weaker. As judged from the ratio between  $H\alpha$  and  $[NII]\lambda 6853$ , the gas metallicity of ASK 25 is smaller.

- ASK 27 spectrum is very similar to that of ASK 25.

In order to carry out the comparison of this qualitative analysis with the quantitative analysis in Sect. 5, we define a *stellar age index* that sorts the ASK classes according to the age of their stellar populations. The stellar age index (SAI) is defined as follows. Based on the absorption lines in the region containing the UV breaks and the UV continuum, we order the ASK classes according to their relative stellar ages. For instance, having stronger broader Balmer lines implies being older. Since the ordering is rough, we allow for several classes to share the

same age bin. Once the order has been set, we assign a sequential number to this order from the older stellar population  $\text{SAI}=0$  (ASK 0) to the youngest stellar population  $\text{SAI}=13$  (ASK 20). The SAI thus defined qualitatively orders the stellar populations from the oldest to the youngest, although it does not assign specific ages to the ASK classes. SAIs are included in Table 1.

Similarly, a gas metallicity index (GMI) is defined to sort the classes according to their gas-phase metallicities. In this case we use the N2 index, i.e.,  $\log([\text{NII}]\lambda 6583/\text{H}\alpha)$ , which is a well known proxy for gas metallicity (see item # 7 in Sect. 3.1). Again, the index (i.e., N2 renamed as GMI) is listed among the properties of the classes in Table 1. GMI is used for comparison with the quantitative analysis described in Sect. 6.

## 5. QUANTITATIVE ANALYSIS OF THE STELLAR POPULATIONS USING STARLIGHT

We use the star formation histories (SFH) derived using the code STARLIGHT (Cid Fernandes et al. 2005; Asari et al. 2007) to cross-check the qualitative analysis carried out in the previous sections. STARLIGHT decomposes the observed absorption spectrum in terms of a sum of single stellar populations (SSP), i.e., coeval starbursts with an assumed initial mass function, a common metallicity (*the metallicity*), and observed with a time-lag with respect to the burst (*the age*). Each SSP produces a known spectrum, and a linear combination of these spectra is fitted to the observed spectrum, being the amplitudes applied to each SSP the free parameters of the fit. Extinction is modeled as a foreground dust screen, with its wavelength dependence given by the extinction law of Calzetti et al. (1994), and then scaled during the fitting process using a single degree of freedom. (Other extinction laws were tried and yield equivalent results; see Asari et al. 2007.) The amplitudes of the SSPs represent the measured SFH. STARLIGHT uses the Metropolis scheme to carry out the  $\chi^2$  minimization (for a full description of the code, see Cid Fernandes et al. 2005). The amplitudes thus derived are proportional to the fraction of the galaxy mass produced by each individual SSP burst, and they are the parameters used in our study (after suitable normalization to 100). In our particular rendering, STARLIGHT employs 150 SSPs from Bruzual & Charlot (2003), combined according to the Padova 1994 evolutionary tracks (Girardi et al. 1996, and references therein). The SSPs cover a grid of 6 metallicities (from 0.005 to 2.5 times solar) and 25 ages (from 1 Myr to 18 Gyr). Further details are given in Sect. 2.1 of Asari et al. (2007). Under these assumptions, we computed the SFH of each galaxy with a spectrum in SDSS-DR7.

Figure 16 shows mean SFHs for a number of representative ASK classes. The average considers all the SDSS-DR7 galaxies in each ASK class. The classes have been chosen so that they cover the full range of possibilities, from the oldest reddest stellar populations (ASK 0) to the youngest bluest ones (ASK 20). ASK 5, 14 and 18 illustrate intermediate cases. Figure 17 is equivalent to Fig. 16 except that, rather than mass, it shows the percentage of present light (at 4020 Å) produced by each one of the SSPs. Note how light is strongly biased towards young populations, as compared to mass which is held by old populations. The dotted lines in the fig-

ure represent  $\pm$  one standard deviation considering all the galaxies in SDSS-DR7 corresponding to a given ASK class. These are the histograms used to compute the luminosity-weighted averages and dispersions discussed in the next paragraph.

Figure 18a shows the relationship between the mean luminosity-weighted age as derived from STARLIGHT and the estimate of relative age carried out in Sect. 4 (SAI). The error bars give the rms fluctuations among the ages of the SSPs that contribute to each class. The correlation age-SAI is extremely good, implying that our quick qualitative estimate is consistent with the detailed up-to-date modeling. Moreover, the existence of an almost one-to-one correlation provides specific timescales to our qualitative dating. SAI between 0 and 2 correspond to a single old metal rich population, with ages between 11.2 and 6.7 Gyr (see the SFH for ASK 0 in Fig 16). SAI between 3 and 7 has two stellar populations assigned, one old and one young (Table 1). They have mean ages between 7.4 Gyr and 1.2 Gyr. Finally, from SAI 8 onwards, we qualitatively find young populations, and their mean STARLIGHT ages go from 250 Myr to 5 Myr.

Figure 18b displays the mean stellar metallicity corresponding to each SAI. The metallicity is high (slightly super-solar) when  $\text{SAI} \leq 2$ , i.e., in the classes our qualitative analysis catalogued as having old stellar populations. In this case the scatter is fairly small (see the error bars in the figure), meaning that all their old stars are metal-rich. The scatter increases and the mean metallicity decreases for younger populations. We interpret this result as an increase of the number of stellar populations that contribute to the galaxy spectra, which is corroborated by the SFHs of ASK 5, 14 and 18 in Fig. 16 (with SAI 3, 7 and 8, respectively). The stellar metallicity grows slightly for spectra corresponding to even younger stellar populations, and it becomes slightly sub-solar for the youngest ASK classes. The scatter remains large, also reflecting the significant number of stellar components in these galaxies.

## 6. QUANTITATIVE ANALYSES OF THE EMISSION LINE SPECTRA

One of the most sophisticated techniques of analysis of ionized nebulae involves measuring emission-line fluxes of many atomic species to derive their relative abundances. Adding up all the ionization states of an element provides its abundance. This approach is the so-called direct method or temperature-based method. The fluxes depend on atomic parameters as well as on the physical conditions of the plasma (e.g., Pagel & Edmunds 1981; Osterbrock 1989; Shields 1990; Stasińska 2004). Once the atomic parameters are known (or assumed), one can use the observed lines to retrieve, simultaneously, the elemental abundances and the physical conditions of the nebula. For instance, using collisional excited lines of the same species having different excitation potentials, one can determine the electron temperature (e.g.,  $[\text{OIII}]\lambda 4363$  and  $[\text{OIII}]\lambda 5007$ ). Similarly, lines of the same species with the same excitation potential but different collisional de-excitation rates, provide diagnostics for the electron density (e.g.,  $[\text{SII}]\lambda 6731$  to  $[\text{SII}]\lambda 6717$ ). We have applied this technique to determine the oxygen abundance characteristic of the emission lines of the ASK classes that are starbursts. The ac-

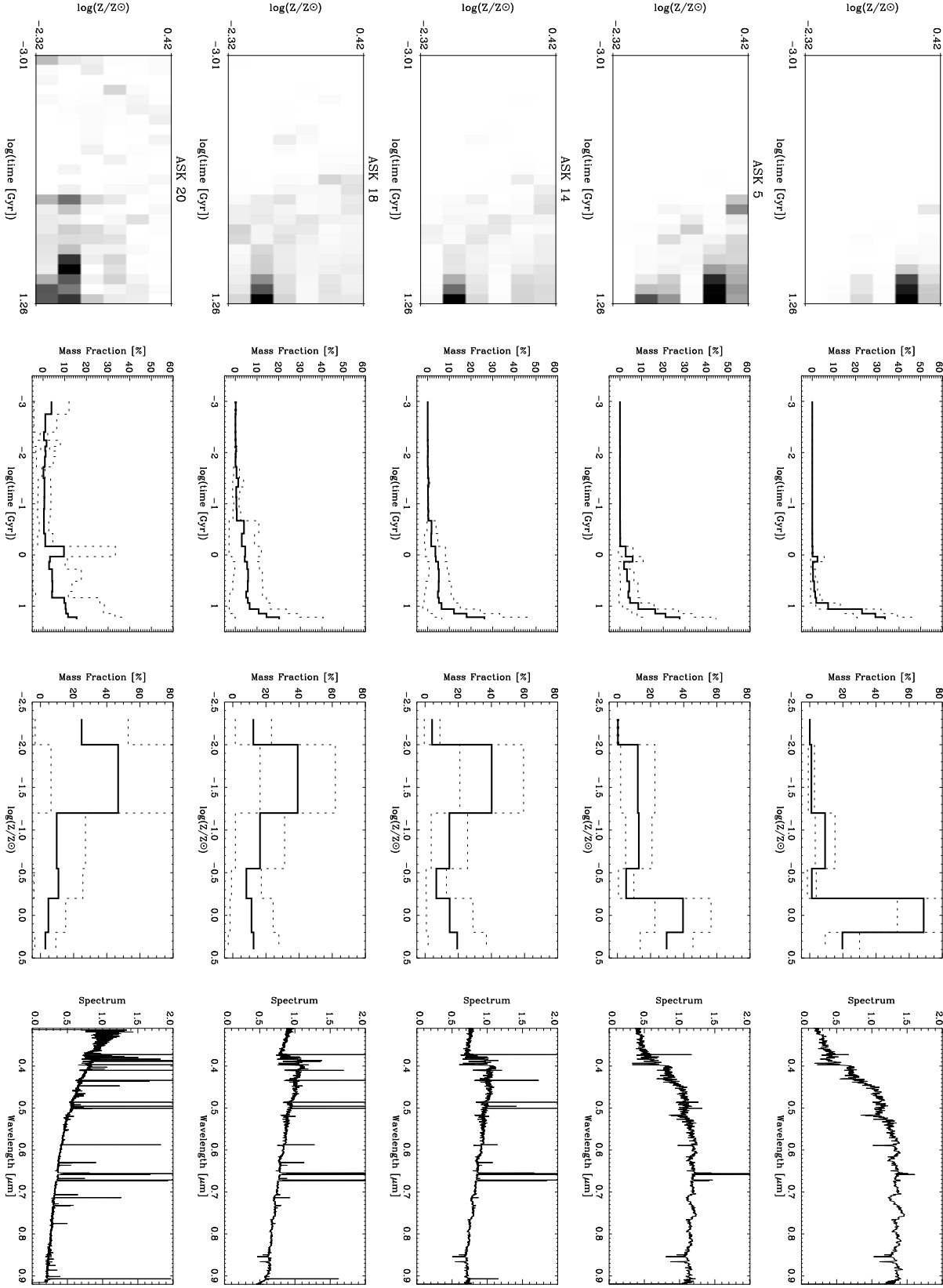


FIG. 16.— (The figure must be rotated by  $90^\circ$ .) Each row corresponds to a particular ASK class as indicated. First column: SFHs derived from the application of STARSIGHT to spectra of individual galaxies, which are then averaged according to their classes. The classes on display have been chosen so that they cover the full range of possibilities, from the oldest reddest stellar populations (ASK 0) to the youngest bluest ones (ASK 20). ASK 5, 14 and 18 represent intermediate cases. The SFHs are two dimensional functions with the abscissae representing look-back time, and the ordinates metallicity. The scale of grays goes from maximum to minimum. Second column: the solid lines show the average of the SFHs along the metallicity axes. The dotted lines correspond to  $\pm$  one standard deviation from the average considering all the galaxies included in a given ASK class. Third column: same as the second column except that the average of the SFHs is carried out along the time axes. The spectrum of each ASK class is also shown for reference in the fourth column.

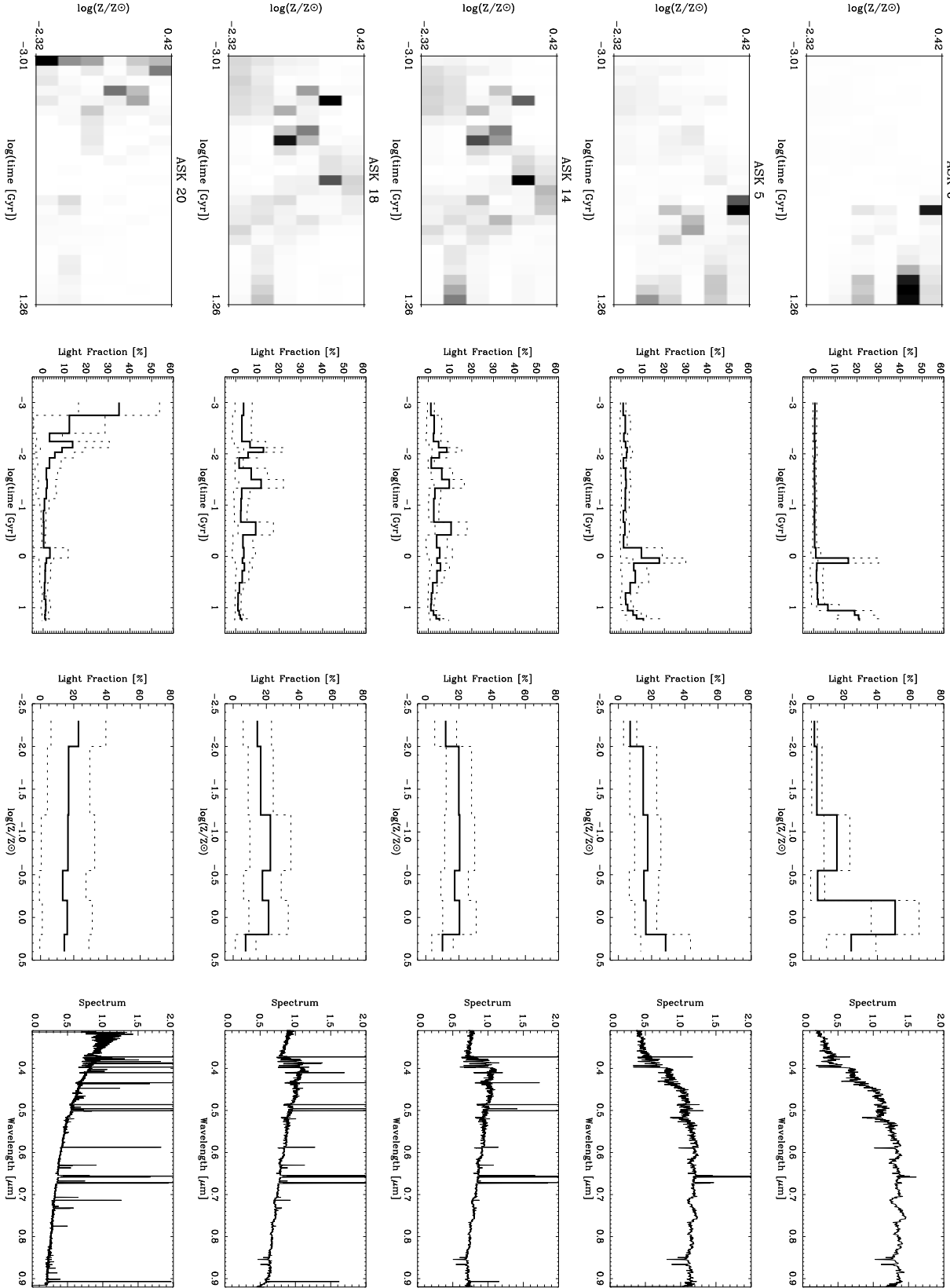


FIG. 17.— (The figure must be rotated by  $90^\circ$ .) Percentage of light corresponding to each one of the SSPs (first column), and its projection in the age axis (second column), and in the metallicity axis (third column). Same as Fig. 16, except that the mass of each component has been weighted by the corresponding light-to-mass ratio. The ASK classes have been chosen to represent the full range of possibilities, and they are the same as those in Fig. 16. See the caption of Fig. 16 for further details.

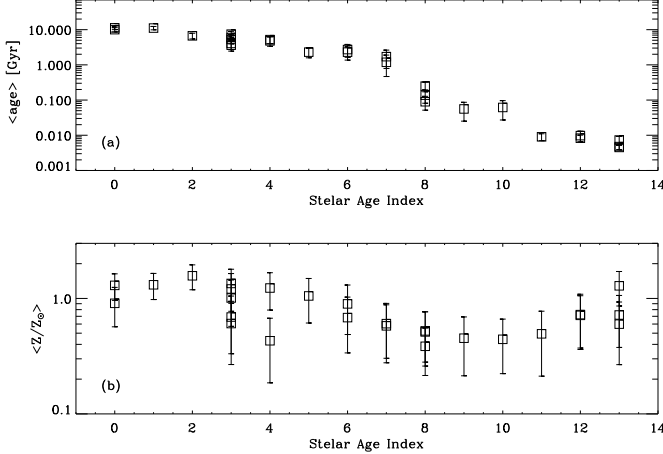


FIG. 18.— (a) Mean light-weighted age as derived from STARLIGHT vs SAI (stellar age index). Note the tight correlation. (b) Mean metallicity  $Z$  derived from STARLIGHT vs SAI. The error bars give the rms fluctuations among the ages and metallicities of the SSPs included in each class. The scatter of metallicities is large except for  $\text{SAI} \leq 2$ . As usual,  $Z_{\odot}$  stands for the solar metallicity.

tual recipe is described by Pérez-Montero & Díaz (2003) and Hägele et al. (2008), and it has been widely used (e.g., Amorín et al. 2010, 2012). We refer to the original references for details on the technique and atomic parameters. Whenever possible, the electron temperature was inferred from  $[\text{OIII}]\lambda 4363$ . This line weakens with increasing metallicity, therefore, it cannot be used with the classes of large metallicities (see item # 8 in Sect. 3.1). The problem was bypassed in these cases using  $[\text{SIII}]\lambda 6312$  and  $[\text{SIII}]\lambda 9069$  to derive the sulphur electron temperature, which was then used for oxygen after scaling (Hägele et al. 2006). ASK classes 17, 20, 21, 22, 24, 25, 26, and 27 have  $[\text{OIII}]\lambda 4363$  intense enough to determine electron temperatures. The line is not detectable in classes 12, 14, 16, 18, 19 and 23, however they show  $[\text{SIII}]\lambda 6312$ , which we used for deriving electron temperatures. Finally, classes ASK 10, 11 and 13 do not allow us to measure either  $[\text{OIII}]\lambda 4363$  or  $[\text{SIII}]\lambda 6312$ , and so we could not assign an oxygen abundance using the direct method. Classes 20, 21, 22, 24, 25, 26, and 27 allow to determine electron temperatures from both  $[\text{OIII}]\lambda 4363$  and  $[\text{SIII}]\lambda 6312$ . The oxygen abundances obtained using the two ways of estimating temperature agree within  $\pm 0.02$  dex. All the abundances thus obtained are listed in Table 1.

As we explain in Sect. 4, the metallicity of the gaseous component of the template spectra was judged based on the ratio between  $[\text{NII}]\lambda 6583$  and  $\text{H}\alpha$ . This ratio is therefore our qualitative metallicity index (Table 1), which is compared with the direct oxygen abundance in Fig. 19. The correlation is extremely good, at least from solar metallicity ( $\log[\text{O}/\text{H}]_{\odot} = 8.69 \pm 0.05$ ; Asplund et al. 2009) to one tenth the solar value. The fluctuations of the actual data with respect to a linear fit are just 0.06 dex, which is significantly smaller than the same correlation obtained from individual galaxies – e.g., Pettini & Pagel (2004) claim 0.2 dex. From the very good correlation between oxygen abundance and  $[\text{NII}]\lambda 6583/\text{H}\alpha$  we conclude that the qualitative analysis of nebular metallicities is consistent with the quantitative

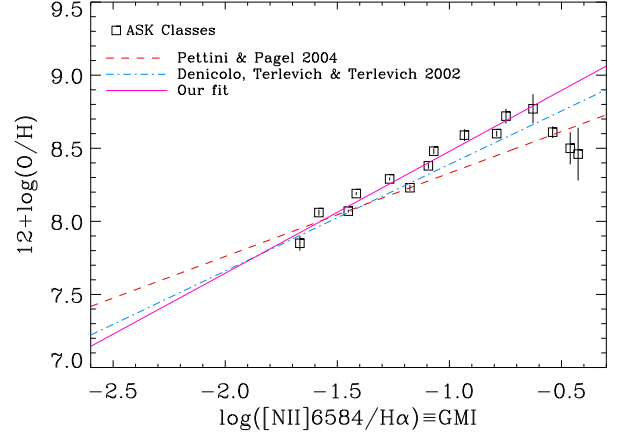


FIG. 19.— Oxygen abundance of the emission-line component of the templates. They have been computed as precisely as possible through estimation of electron temperatures. The oxygen abundance is represented versus the ratio  $[\text{NII}]\lambda 6583$  to  $\text{H}\alpha$ , which is the proxy used to estimate the metallicity in our qualitative scheme. Error bars are computed in a Monte-Carlo simulation to be consistent with the errors assigned to the observed fluxes. The straight lines correspond to various estimates of the relationship from individual galaxies and HII regions by Denicoló et al. (2002, the dotted-dashed line) and by Pettini & Pagel (2004, the dashed line), and from our ASK templates (the solid line). Our linear fit excludes the three rightmost points, and it reads,  $12 + \log(\text{O}/\text{H}) = (0.83 \pm 0.05) \times \log([\text{NII}]\lambda 6583/\text{H}\alpha) + (9.31 \pm 0.07)$ .

estimate using the best techniques available.

## 7. ADDITIONAL RESULTS AND DISCUSSIONS

Figure 20a shows the index used to determine the gas metallicity,  $\log[\text{NII}]\lambda 6583/\text{H}\alpha$ , vs the index used to characterize the age of the stellar populations, SAI. It is clear that the two indices are correlated, indicating that the templates with the lowest oxygen content also have the youngest stellar populations. This is explicitly shown in Fig. 20b, which presents the same kind of relationship but using quantitative determinations of ages and gas-phase metallicities. (The two last points deviating from the linear relationship will be ignored since the trend they represent is not present in Fig. 20a, and they have particularly weak  $[\text{OIII}]\lambda 4363$  lines, with the uncertainties that this entails – see item # 8 in Sect. 3.1.) The correlation is similar to that found by Fernandes et al. (2003). The physical origin of the relationship is unclear. It may be a side-effect of the galaxy mass (a phenomenon often referred to as downsizing; see, e.g., Neistein et al. 2006). First, the mass-metallicity relationship implies that low-mass galaxies are less metallic (e.g., Skillman et al. 1989). Second, the mass-age relationship (e.g., Heavens et al. 2004) implies that low-mass galaxies also have younger stellar populations. Finally, the bluest ASK classes contain more dwarf galaxies (Sánchez Almeida et al. 2010), therefore, they are less metallic and with younger stars, giving as a side-effect the observed correlation. Even though this explanation is feasible, the relationship between gas-metallicity and stellar-age shown in Figs. 20 is so clean that it looks fundamental rather than derived from the combined effect of two other relationships. This conjecture is supported by the scatter plots in Fig. 21, that include the two variables involved in Fig. 20b plus the galaxy mass. Assigning

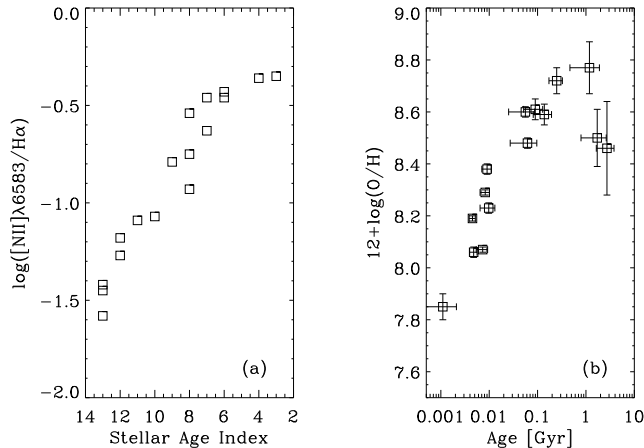


FIG. 20.— (a) Scatter plot of the index used to determine the gas metallicity,  $\log[\text{NII}]\lambda 6583/\text{H}\alpha$ , vs the index used to characterize the age of the stellar populations, SAI. They are correlated. (b) Same representation as (a) but using quantitative determinations of gas metallicity and age. The age of the point corresponding to ASK 15 (i.e., the youngest class with the lowest oxygen content) is just an upper limit, which we include to show that the relationship continues to the youngest targets.

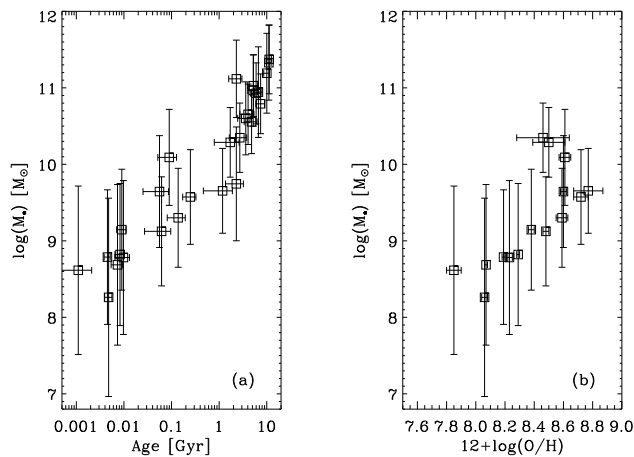


FIG. 21.— (a) Scatter plot of the mass of the galaxies in each ASK class versus the mean stellar age. The vertical error bars represent the standard deviation among all the individual galaxies in each class. The horizontal error bars are the same as in Fig. 20b. (b) Scatter plot of the mass of the galaxies in a class versus the gas-phase metallicity. The error bars have the same meaning as in panel (a).

masses to the ASK templates is not without ambiguity, since the spectra of the individual galaxies were normalized before averaging (Sect. 2). However, we computed the mean and standard deviation among the masses of all the galaxies in each ASK class<sup>8</sup>, and those are the masses assigned to the classes in Figs. 21. One can see that the templates follow a mass-metallicity relationship (Fig. 21b) and a mass-age relationship (Fig. 21a), but both are less tight than the metallicity-age relationship in Fig. 20b, which seems to be the primary relationship.

In short, the properties of the gas and the stars are

<sup>8</sup> Stellar masses derived from integrated magnitudes using color-dependent mass-to-light ratios from Bell & de Jong (2001).

not independent but tightly correlated in real galaxies. Galaxy mass does not seem to be the only factor driving such correlation.

Galaxy spectra seem to follow a 1D sequence, with a secondary branch for AGNs (Connolly et al. 1995; Yip et al. 2004; Vanderplas & Connolly 2009; Ascasibar & Sánchez Almeida 2011). In other words, an independent parameter (affine parameter) characterizes most properties of galaxy spectra, from the red passive ones to those actively forming stars. The actual nature of the affine parameter is unknown, but the results in this paper suggest it to be the mean age of the stellar population. The ASK templates can be naturally ordered by mean stellar age (or by SAI, in our parlance), and the order thus obtained turns out to be extremely similar to the one obtained using minimal spanning trees by Ascasibar & Sánchez Almeida (2011). The latter represents a non-trivial exercise to find the location of the templates in the 1637-dimensional space where the ASK classification was carried out (i.e., a space where each galaxy is a point, and the 1637 coordinates represent the flux at particular wavelengths). They are organized in a 1D sequence with the same order given by the luminosity-weighted mean stellar age. We take the agreement between the two orderings as a strong suggestion that stellar age is the affine parameter. Note that the emission line spectrum is prominent in blue galaxies and so it plays a major role in shaping the galaxy spectra. That fact that the spectrum of a galaxy is (mostly) dictated by the age of the stellar population implies that the emission lines and the absorption lines are not independent. This is indeed the conclusion reached in the previous paragraph through a totally different argument.

We argued in Sect. 2 that the ASK classes are representative of all local galaxies since they condense the properties of some one million galaxies of the local universe. Even though we endorse the statement, it must be clarified. ASK templates are representative of the most common galaxies, however, some important but uncommon galaxies are not included. In particular, the most massive galaxies that dominate the centers of galaxy clusters (brightest cluster galaxies and cD galaxies) are not properly described. These massive red galaxies have old stellar populations so they are classified as ASK 0 and ASK 2 (Aguirri et al. 2012). However, they represent a small fraction of all the galaxies in these classes, so that their contribution to the average (template) spectra of ASK 0 and 2 is negligible. The same may happen with other kinds of rare objects like BL Lac (e.g., Stein et al. 1976), objects with extreme star formation rates (e.g., Cardamone et al. 2009), extremely metal poor galaxies (e.g., Morales-Luis et al. 2011), and others. The fact that some objects may escape the simplified schematic in Sect. 3.2 do not invalidate the analysis – it will be useful to indicate that these objects are unusual.

The comparison between Figs. 16 and 17 evidences a fact that is well documented in the literature, but which still results somewhat surprising. Most galaxies formed a significant fraction of their stellar mass long ago when the universe was just a few Gyr old, even those forming stars today (e.g., Heavens et al. 2004; Asari et al. 2007; Dunlop 2011). This fact is obviously true for ASK classes representing passively evolving red galaxies (see ASK 0 in Fig. 16), but it also holds true for young ASK classes – see

the important contribution of old stellar populations to the ASK 20 SFH in Fig. 16, even though its luminosity-weighted mean age is just 4.5 Myr (Table 1). When the mass contribution is transformed to light contribution (Fig. 17), it becomes clear how newborn stars outshine the older populations, that are heavily underrepresented in the composite galaxy spectrum. If a galaxy happens to undergo a significant starburst, spectrum-wise it looks young.

There is a conspicuous difference between the old stellar populations present in passively evolving galaxies and in star-forming galaxies. The metallicity of the old stars is high in passive galaxies and very low in starbursts (compare the SFHs of ASK 0 and ASK 20 in the first column of Fig. 16). The dominance of old metal rich stellar populations in red galaxies is well known (e.g., Renzini 2006), so does the fact that the old stars in dwarf galaxies of the local group have extremely low metallicity (e.g., Miller et al. 2001; Monelli et al. 2010; Hidalgo et al. 2011).

## 8. CONCLUSIONS

As argued in the introduction, we have sophisticated computer codes for inferring the properties of the stellar populations contributing to the observed galaxy spectra. Similarly, tools are available for qualitative diagnostics of the physical properties of the galaxy gas. They have been developed by specialist groups, and then kindly offered to a much broader community. Technicalities often complicate the interpretation of the results, therefore, there is a natural tendency to apply these sophisticated tools in black-box fashion, which turns out to be quite unsatisfactory for a physical stand point. One obtains a detailed description of the stars and gas producing the observed galaxy spectra, but overlooks the reasons why the computer code has preferred them rather than other alternatives. We provide a simple step-by-step guide to qualitative interpretation of galaxy spectra. It is not precise, and has not been planned as an alternative to the existing tools. However, it allows a quick-look that yields the main properties of the spectra in a intuitive fashion. This may be of interest in various applications, e.g., to provide physical insight when using sophisticated tools, or to interpret noisy spectra. Moreover, the results of the qualitative analysis agree with those inferred using up-to-date computer codes.

The step-by-step guide is described in Sect. 3.2, and it has been summarized as a simple questionnaire in Fig. 11. Emission and absorption lines are analyzed separately, which give rise to a classification with one entry for the gas and another for the stars. (In real galaxies, however,

the properties of gas and stars are tightly correlated; see Sect. 7.) The analysis has been systematically applied to the set of ASK template spectra that resulted from the classification of all galaxy spectra in SDSS-DR7 (see Sect. 2). Their physical properties are summarized in Table 1. With the caveats pointed out in Sect. 7, the ASK classes represent a comprehensive set of galaxy spectra, that go all the way from passively evolving red galaxies (e.g., ASK 0) to HII galaxies, dominated by massive newborn stars having no absorption lines (e.g., ASK 15). Since it works for this set, the analysis should work for most galaxies.

The qualitative analysis is found to be in excellent agreement with quantitative numerical codes. We show how the index for stellar-age (SAI) follows an almost one-to-one correlation with the mean stellar age assigned by the code STARLIGHT (Fig. 18). Similarly, we found how the proxy for gas metallicity is in good agreement with the (oxygen) metallicity inferred by applying the direct method to the emission lines of the ASK templates (Fig. 19).

The ASK templates are freely available (see footnote # 6) and, together with their physical properties listed in Table 1, they can be used as benchmarks so that any other galaxy spectrum can be analyzed by reference to them.

Thanks are due to C. Ramos Almeida and E. Pérez-Montero for discussions and help with references. This work has been funded by the Spanish MICIN project *Estalidos*, AYA 2010-21887-C04-04. ET and RT acknowledge also financial support by the Mexican Research Council (CONACYT), through grants CB-2005-01-49847, 2007-01-84746 and 2008-103365-F. We are members of the Consolider-Ingenio 2010 Program, grant MICINN CSD2006-00070: First Science with GTC. Funding for the SDSS and SDSS-II has been provided by the Alfred P. Sloan Foundation, the Participating Institutions, the National Science Foundation, the U.S. Department of Energy, the National Aeronautics and Space Administration, the Japanese Monbukagakusho, the Max Planck Society, and the Higher Education Funding Council for England. The SDSS is managed by the Astrophysical Research Consortium for the Participating Institutions (for details, see the SDSS web site at <http://www.sdss.org/>). The STARLIGHT project is supported by the Brazilian agencies CNPq, CAPES and FAPESP and by the France-Brazil CAPES/Cofecub program.

*Facilities:* Sloan (DR7, spectra)

## REFERENCES

- Abazajian, K. N., Adelman-McCarthy, J. K., Agüeros, M. A., et al. 2009, *ApJS*, 182, 543  
 Aguerri, J. A. L., Huertas-Company, M., Sánchez Almeida, J., & Muñoz-Tuñón, C. 2012, *A&A*, 540, A136  
 Allard, F., Hauschildt, P. H., & Schwenke, D. 2000, *ApJ*, 540, 1005  
 Allen, M. G., Groves, B. A., Dopita, M. A., Sutherland, R. S., & Kewley, L. J. 2008, *ApJS*, 178, 20  
 Alloin, D., Collin-Souffrin, S., Joly, M., & Vigroux, L. 1979, *A&A*, 78, 200  
 Amorín, R., Pérez-Montero, E., Vílchez, J. M., & Papaderos, P. 2012, *ApJ*, 749, 185  
 Amorín, R. O., Pérez-Montero, E., & Vílchez, J. M. 2010, *ApJ*, 715, L128  
 Arétxaga, I., Terlevich, E., Terlevich, R. J., Cotter, G., & Díaz, Á. I. 2001, *MNRAS*, 325, 636  
 Asari, N. V., Cid Fernandes, R., Stasińska, G., et al. 2007, *MNRAS*, 381, 263  
 Ascasibar, Y. & Sánchez Almeida, J. 2011, *MNRAS*, 415, 2417  
 Asplund, M., Grevesse, N., Sauval, A. J., & Scott, P. 2009, *ARA&A*, 47, 481  
 Baldwin, J. A., Phillips, M. M., & Terlevich, R. 1981, *PASP*, 93, 5  
 Bell, E. F. & de Jong, R. S. 2001, *ApJ*, 550, 212  
 Bishop, C. M. 2006, *Pattern Recognition and Machine Learning* (NY: Springer)  
 Bruzual, G. & Charlot, S. 2003, *MNRAS*, 344, 1000

- Calzetti, D., Kinney, A. L., & Storchi-Bergmann, T. 1994, *ApJ*, 429, 582
- Cardamone, C., Schawinski, K., Sarzi, M., et al. 2009, *MNRAS*, 399, 1191
- Cenarro, A. J., Gorgas, J., Cardiel, N., Vazdekis, A., & Peletier, R. F. 2002, *MNRAS*, 329, 863
- Chen, Y.-M., Tremonti, C. A., Heckman, T. M., et al. 2010, *AJ*, 140, 445
- Cid Fernandes, R., Gu, Q., Melnick, J., et al. 2004, *MNRAS*, 355, 273
- Cid Fernandes, R., Mateus, A., Sodré, L., Stasińska, G., & Gomes, J. M. 2005, *MNRAS*, 358, 363
- Cid Fernandes, R., Stasińska, G., Mateus, A., & Vale Asari, N. 2011, *MNRAS*, 413, 1687
- Cid Fernandes, R., Stasińska, G., Schlickmann, M. S., et al. 2010, *MNRAS*, 403, 1036
- Ciddor, P. E. 1996, *Appl. Opt.*, 35, 1566
- Connolly, A. J., Szalay, A. S., Bershad, M. A., Kinney, A. L., & Calzetti, D. 1995, *AJ*, 110, 1071
- Denicoló, G., Terlevich, R., & Terlevich, E. 2002, *MNRAS*, 330, 69
- Díaz, A. I. & Pérez-Montero, E. 2000, *MNRAS*, 312, 130
- Díaz, A. I., Terlevich, E., & Terlevich, R. 1989, *MNRAS*, 239, 325
- Dunlop, J. S. 2011, *Science*, 333, 178
- Everitt, B. S. 1995, *Cluster Analysis* (London: Arnold)
- Fernandes, R. C., Leão, J. R. S., & Lacerda, R. R. 2003, *MNRAS*, 340, 29
- Flores-Fajardo, N., Morisset, C., Stasińska, G., & Binette, L. 2011, *MNRAS*, 415, 2182
- Giovanelli, R., Haynes, M. P., Salzer, J. J., et al. 1994, *AJ*, 107, 2036
- Girardi, L., Bressan, A., Chiosi, C., Bertelli, G., & Nasi, E. 1996, *A&AS*, 117, 113
- González Delgado, R. M., Leitherer, C., & Heckman, T. M. 1999, *ApJS*, 125, 489
- Goulding, A. D. & Alexander, D. M. 2009, *MNRAS*, 398, 1165
- Hägele, G. F., Díaz, Á. I., Terlevich, E., et al. 2008, *MNRAS*, 383, 209
- Hägele, G. F., Pérez-Montero, E., Díaz, Á. I., Terlevich, E., & Terlevich, R. 2006, *MNRAS*, 372, 293
- Hamilton, D. 1985, *ApJ*, 297, 371
- Heavens, A., Panter, B., Jimenez, R., & Dunlop, J. 2004, *Nature*, 428, 625
- Heckman, T. M. 1980, *A&A*, 87, 152
- Hidalgo, S. L., Aparicio, A., Skillman, E., et al. 2011, *ApJ*, 730, 14
- Johnson, M. D., Levitt, J. S., Henry, R. B. C., & Kwitter, K. B. 2006, in *IAU Symposium, Vol. 234, Planetary Nebulae in our Galaxy and Beyond*, ed. M. J. Barlow & R. H. Méndez, 439–440
- Jørgensen, I. 1999, *MNRAS*, 306, 607
- Kauffmann, G., Heckman, T. M., Tremonti, C., et al. 2003, *MNRAS*, 346, 1055
- Kewley, L. J., Groves, B., Kauffmann, G., & Heckman, T. 2006, *MNRAS*, 372, 961
- Koleva, M., Prugniel, P., Bouchard, A., & Wu, Y. 2009, *A&A*, 501, 1269
- Luridiana, V., Shaw, R. A., & Morisset, C. 2011, in *IAU Symp., Vol. 283, Planetary Nebulae: An Eye to the Future*, ed. A. Manchado & L. Stanghellini (Cambridge: Cambridge University Press), in press – check
- Maeder, A., Lequeux, J., & Azzopardi, M. 1980, *A&A*, 90, L17
- Mas-Hesse, J. M. & Kunth, D. 1999, *A&A*, 349, 765
- Massaro, E., Nesci, R., & Piranomonte, S. 2012, *MNRAS*, 422, 2322
- Massey, P. 2002, *ApJS*, 141, 81
- Masters, K. L., Nichol, R., Bamford, S., et al. 2010, *MNRAS*, 404, 792
- McGaugh, S. S. 1991, *ApJ*, 380, 140
- Miller, B. W., Dolphin, A. E., Lee, M. G., Kim, S. C., & Hodge, P. 2001, *ApJ*, 562, 713
- Monelli, M., Gallart, C., Hidalgo, S. L., et al. 2010, *ApJ*, 722, 1864
- Morales-Luis, A. B., Sánchez Almeida, J., Aguerri, J. A. L., & Muñoz-Tuñón, C. 2011, *ApJ*, 743, 77
- Neistein, E., van den Bosch, F. C., & Dekel, A. 2006, *MNRAS*, 372, 933
- Ocvirk, P., Pichon, C., Lançon, A., & Thiébaud, E. 2006, *MNRAS*, 365, 74
- Osterbrock, D. E. 1989, *Astrophysics of gaseous nebulae and active galactic nuclei*
- Pagel, B. E. J. & Edmunds, M. G. 1981, *ARA&A*, 19, 77
- Pagel, B. E. J., Edmunds, M. G., Blackwell, D. E., Chun, M. S., & Smith, G. 1979, *MNRAS*, 189, 95
- Panther, B., Heavens, A. F., & Jimenez, R. 2004, *MNRAS*, 355, 764
- Pérez-Montero, E. & Díaz, A. I. 2003, *MNRAS*, 346, 105
- Pettini, M. & Pagel, B. E. J. 2004, *MNRAS*, 348, L59
- Renzini, A. 2006, *ARA&A*, 44, 141
- Reunanen, J., Kotilainen, J. K., & Prieto, M. A. 2003, *MNRAS*, 343, 192
- Rodríguez-Ardila, A., Prieto, M. A., Portilla, J. G., & Tejeiro, J. M. 2011, *ApJ*, 743, 100
- Sánchez Almeida, J., Aguerri, J. A. L., Muñoz-Tuñón, C., & de Vicente, A. 2010, *ApJ*, 714, 487
- Sánchez Almeida, J., Aguerri, J. A. L., Muñoz-Tuñón, C., & Huertas-Company, M. 2011, *ApJ*, 735, 125
- Sánchez-Janssen, R., Amorín, R., & et al. 2012, *A&A*, submitted
- Schaerer, D., Contini, T., & Pindao, M. 1999, *A&AS*, 136, 35
- Schneider, D. P., Hall, P. B., Richards, G. T., et al. 2007, *AJ*, 134, 102
- Shaw, R. A. & Dufour, R. J. 1995, *PASP*, 107, 896
- Shi, F., Kong, X., Li, C., & Cheng, F. Z. 2005, *A&A*, 437, 849
- Shields, G. A. 1990, *ARA&A*, 28, 525
- Shirazi, M. & Brinchmann, J. 2012, *MNRAS*, 421, 1043
- Skillman, E. D., Kennicutt, R. C., & Hodge, P. W. 1989, *ApJ*, 347, 875
- Stasińska, G. 2004, in *Cosmochemistry. The melting pot of the elements*, ed. C. Esteban, R. García López, A. Herrero, & F. Sánchez, 115–170
- Stein, W. A., Odell, S. L., & Strittmatter, P. A. 1976, *ARA&A*, 14, 173
- Stoughton, C., Lupton, R. H., Bernardi, M., et al. 2002, *AJ*, 123, 485
- Tojeiro, R., Heavens, A. F., Jimenez, R., & Panter, B. 2007, *MNRAS*, 381, 1252
- Vanderplas, J. & Connolly, A. 2009, *AJ*, 138, 1365
- Vazdekis, A., Casuso, E., Peletier, R. F., & Beckman, J. E. 1996, *ApJS*, 106, 307
- Worthey, G., Faber, S. M., Gonzalez, J. J., & Burstein, D. 1994, *ApJS*, 94, 687
- Yan, R. & Blanton, M. R. 2012, *ApJ*, 747, 61
- Yip, C. W., Connolly, A. J., Szalay, A. S., et al. 2004, *AJ*, 128, 585